Diversity and assembly of active bacteria and their potential function along soil aggregates in a paddy field

Authors

Chenxiao Ding[a], Xinji Xu[a], Yaowei Liu[a], Xing Huang[a], MengYuan Xi[b], Haiyang Liu[c], Elizabeth Deyett[b], Marc G. Dumont[d], Hongjie Di[a], Marcela Hernández[e], Jianming Xu[a], Yong Li[a*]

Affiliations and addresses

[a]Zhejiang Provincial Key Laboratory of Agricultural Resources and Environment, College of Environmental and Resource Sciences, Zhejiang University, Hangzhou 310058, China

[b]Department of Botany and Plant Sciences, University of California, Riverside 92521, USA

[c]College of Resources and Environment, Henan Agricultural University, Zhengzhou 450002, China

[d] School of Biological Sciences, University of Southampton, Southampton, SO17 1BJ, UK

[e]School of Biological Sciences, University of East Anglia, Norwich, NR4 7TJ, UK

***Corresponding author:** Yong Li (E-mail: liyongcn@zju.edu.cn)

Abstract:

Numerous studies have found that soil microbiomes differ at the aggregate level indicating they provide spatially heterogeneous habitats for microbial communities to develop. However, an understanding of the assembly processes and the functional profile of microbes at the aggregate level remain largely rudimentary, particularly for those active members in soil aggregates. In this study, we investigated the diversity, co-occurrence network, assembly process and predictive functional profile of active bacteria in aggregates of different sizes using $H_2{}^{18}O$-based DNA stable isotope probing (SIP) and 16S rRNA gene sequencing. Most of the bacterial reads were active with 91% of total reads incorporating labelled water during the incubation. The active microbial community belonged mostly of Proteobacteria and Actinobacteria, with a relative abundance of 55.32% and 28.12%, respectively. Assembly processes of the active bacteria were more stochastic than total bacteria, while the assembly processes of total bacteria were more influenced by deterministic processes. Furthermore, many functional profiles such as environmental information processing increased in active bacteria (19.39%) compared to total bacteria (11.22%). After incubation, the diversity and relative abundance of active bacteria of certain phyla increased, such as Proteobacteria (50.70% to 59.95%), Gemmatimonadetes (2.63% to 4.11%), and Bacteroidetes (1.50% to 2.84%). In small macroaggregates (SMA: 0.25-2mm), the active bacterial community and its assembly processes differed from that of other soil aggregates (MA: microaggregates, <0.25mm; LMA: large macroaggregates, 2-4mm). For functional profiles, the relative abundance of important functions, such as amino

acid metabolism, signal transduction and cell motility, increased with incubation days and/or in SMA compared to other aggregates. This study provides robust evidence that the community of active bacteria and its assembly processes in soil aggregates differed from total bacteria, and suggests the importance of dominant active bacteria (such as Proteobacteria) for the predicted functional profiles in the soil ecosystem.

Key Words: active bacteria, aggregates, bacterial composition, assembly processes, functional profiles, stable isotope probing

1. Introduction

Microorganisms are fundamental components of soil ecosystems and contribute significantly to ecosystem processes (Bahram et al., 2018). Although thousands of taxa exist in soil ecosystems, a large proportion of this diversity is composed of dormant or inactive individuals (Del Giorgio and Gasol, 2008; Jones and Lennon, 2010; Luna et al., 2002; Roesch et al., 2007). In order to identify the active microbiome in soil, stable isotope probing (SIP) using $^{13}CH_4$, $^{13}CO_2$, $^{15}NO_2$ and $H_2{}^{18}O$ has been successfully used (Aanderud and Lennon, 2011, Dumont and Hernández, 2019). Compared to ^{13}C- and/or ^{15}N-, $H_2{}^{18}O$-based SIP has three advantages in linking microbial community with their function. Firstly, the addition of a single ^{18}O atom increases the degree of physical separation between labelled and unlabelled fractions during isopycnic centrifugation (Aanderud and Lennon, 2011). Secondly, the pervasive requirement of water for cellular maintenance and biosynthesis enables $H_2{}^{18}O$-SIP to identify all actively growing microorganisms (Schwartz, 2007). Finally, $H_2{}^{18}O$ can identify active microbes

67 in soils without additional material, creating an environment more similar to in situ
68 conditions. Schwartz et al. (2014) found significant differences in the community
69 composition of the heavy and light fractions by using $H_2{}^{18}O$- SIP, and significant non-
70 random phylogenetic distribution was found in ^{18}O-labelling bacteria under anoxic
71 conditions (Coskun et al., 2019). Recently, studies have further revealed that most taxa
72 in soils are metabolically active when incubated with $H_2{}^{18}O$ (Papp et al., 2018a, 2018b).
73 Rice paddy ecosystems constitute the largest wetlands on Earth, and host diverse
74 microbial communities responsible for many important ecosystem functions and
75 services (Leff et al., 2004; Bardgett and Van Der Putten, 2014). The relative
76 contributions of deterministic and stochastic processes in microbial communities can
77 be calculated by null and neutral models (Stegen et al., 2012, 2015; Vellend et al., 2014;
78 Zhou and Ning, 2017) and the driving factors of assembly processes for microbial
79 communities in paddy soil have been discussed (Hou et al., 2020; Liu et al., 2020a)
80 revealing that both deterministic and stochastic processes contribute to the assembly of
81 communities (Chase, 2010; Huber et al., 2020; Ofiteru et al., 2010). Environmental
82 factors are found to mediate niche-based deterministic processes (Tripathi et al., 2018)
83 and determinism has been found to be associated with agriculture and correspond with
84 an increase in soil nutrients in paddy soil, especially for abundant bacterial
85 subcommunities (Hou et al., 2020; Liu et al., 2020a). Some researchers suggest that pH
86 and organic matter content are the main regulators of bacterial community composition
87 in paddy soils (Fierer, 2017; Kuramae et al., 2012).
88 The assembly processes of paddy soil microbial communities are found to be more

deterministic compared to other soils (Li et al., 2021). This is counter intuitive as the basis for neutral theory is stochastic processes, such as ecological drift and dispersal (Hubbell, 2005). Indeed, under frequent flooding that facilitates dispersal, microbial communities in paddy soil are dominated by stochastic processes (Liu et al., 2020a; Liu et al., 2021). Muller et al. (2016) found that the ability to enter and exit from dormancy is a significant determinant of community assembly for bacteria. The importance of dispersal for community assembly depends on the metabolic activity of dispersers in the ecosystem (Wisnoski et al., 2020) and these researchers suggest that the assembly processes of active microbes should be dominated by stochastic processes. Liu et al. (2022a) also showed that the assembly processes of active methane-oxidizing bacteria are governed by stochastic processes. Therefore, that the assembly of active and inactive populations of microorganisms in soils differ and the relative proportion of these microbial pools can influence the overall community assembly characteristics.

The living environment of soil microorganisms is controlled by soil aggregates of different sizes and shapes, which possess different characteristics (Lavelle et al., 2006). Soil characteristics are important factors affecting microbial diversity (Pacchioni et al., 2014). Nutrient availability and physicochemical conditions change with aggregate size, further affecting bacterial communities (Briar et al., 2011; Jiang et al., 2017; Trivedi et al., 2017; Vos et al., 2013). Some studies have shown that the higher contents of organic carbon and nutrients in microaggregates (< 0.25 mm) are associated with higher microbial activity and biomass (Jiang et al, 2013; Yan et al., 2018; Zhang et al., 2013a), while others have found that as aggregates became larger, the biomass and activity of

111 bacteria increases along with soil organic matter (Guo et al., 2008; Helgason et al., 2010;
112 Li et al., 2015; Lin et al, 2019; Zhang et al., 2015). Recently, it has been reported that
113 the 1- to 2- mm aggregate fractions have the most active communities and contain the
114 most nutrients in farmland (Liu et al., 2014; Yang et al., 2017) and the higher organic
115 carbon associated with aggregates of 0.25-2mm positively influences bacterial diversity
116 (Jiang et al., 2011; Kandeler et al., 1999; Yang et al., 2019a). Besides, more stochastic
117 processes of bacterial communities in larger aggregates have been found with less
118 selective pressure (Dong et al., 2021). In contrast, a recent study showed that the
119 assembly processes of bacteria are dominated by environmental selection in soil
120 aggregates, and environmental filtering is enhanced with increasing aggregate size
121 (Liao et al., 2022). The understanding of assembly processes at different aggregates is
122 still under debate. For functional profiles, many predicted functions, such as amino acid
123 metabolism, carbohydrate and other categories have been detected in paddy soils and
124 reveal patterns of these genes will facilitate understanding and prediction of relative
125 functional processes (Bai et al., 2013; Barq et al., 2021; Zhang et al., 2013b). Since soil
126 microorganisms are deeply engaged in biogeochemical processes of nutrients and soil
127 fertility, the functions of different communities are critical (Bai et al., 2017; Philippot
128 et al., 2013; Ofek-Lalzar et al., 2014). Although Han et al. (2021) also found soil carbon
129 and nitrogen level of soil aggregates and microbial functional diversity determined
130 multifunctionality in soil, the functional profiles among aggregates are still unknown.
131 In this study, we explore the active bacterial community, assembly processes, and
132 functional profiles at the soil aggregate level by using $H_2{}^{18}O$ SIP 16S ribosomal RNA

(rRNA) gene sequencing, which improves our understanding of the effect of aggregates on active bacteria and their functions. Paddy soils are developed by long-term flooding, taking advantage of the inherent feature of flooded conditions for an $H_2{}^{18}O$ SIP approach. Based on previous studies, we hypothesize that (1) the assembly processes of active bacteria are more stochastic compared to total bacteria; and (2) the diversity of active bacteria is different among soil aggregates.

2. Materials and methods

2.1. Soil sampling and physicochemical properties

Soil samples were taken from a paddy field at Changxing, Zhejiang province (31°00′ N, 119°55′ E). The paddy field belongs to Hydragric Anthrosol, one of the most representative soils in China. The climate of this region is subtropical, with an annual precipitation of 1309 mm and an annual temperature of 15.6 °C. The dominant plant species is rice with paddy yields twice a year. Soil samples from 0 to 20 cm depth were taken on June 2018 at five random locations within three plots (6×6 m) using a soil core sampling. The five soil cores within each plot were mixed to form a single composite sample, and stored at 4 °C until use. Some soils were air-dried and their physicochemical properties were analyzed. The physicochemical properties of soil were estimated according to methods described previously and were provided in Table S1 (Supplemental materials, Table. S1) (Li et al., 2019; Liu et al., 2019a).

2.2. $H_2{}^{18}O$-labelled incubation and aggregate fractionation

$H_2{}^{18}O$ labelled microcosms were setup as described previously (Schwartz, 2007;

155 Papp et al., 2018a) with minor modifications. Briefly, $H_2{}^{18}O$ (99 atom%, Sigma Aldrich,
156 St. Louis, MO) labelled water (^{18}O) and natural-abundance water (unlabelled control,
157 ^{16}O) were constructed for microcosm incubation. Soils were incubated with $H_2{}^{18}O$
158 ($H_2{}^{16}O$ as control) was as control at 25 °C in the dark with 100% maximum water-
159 holding capacity for 4 days in triplicate. Microcosms were set up in 120-ml serum
160 bottles containing wet soil (~ 6 g dry soil), and then sealed with rubber stoppers and
161 aluminum caps.

162 Sampling took place in triplicate microcosms at day 2 and day 4, while day 0 was
163 used as a control. Soils were prepared under sterile conditions for soil aggregate
164 separation using the previously described "optimal moisture" method to standardize soil
165 water content and minimize disturbance to microbial communities (Bach et al., 2018).
166 Soils were dried for eight hours to reach a stable moisture content (~10%), and the
167 following aggregate fractions were separated by shaking through two sieves (2000 μm
168 and 250 μm): large macroaggregates (> 2000 μm, LMA), small macroaggregates (250-
169 2000 μm, SMA) and microaggregates (< 250 μm, MA), avoiding submersion in water
170 (Jiang et al., 2014). Soils were mixed up and down 60 times every 2 min before passing
171 them through the 2000-μm sieve. The soils passed through the 2000-μm sieve were
172 transferred to the next smaller-sized sieve (250 μm) for further screening, resulting in
173 three aggregate fractions. The aggregate fractions were stored at -80 °C for DNA
174 extraction (Fig. S1).

175 **2.3. Nucleic acid extraction and SIP fractionation**

176 FastDNA SPIN kit for soil (MP Biomedicals; Solon, OH, USA) was used to extract

177 DNA from 0.5g of soil. A Nanodrop® ND-2000 UV-vis spectrophotometer (NanoDrop
178 Technologies, Wilmington, DE, USA) was used to estimate the concentrations and
179 quality of DNA.

180 Bulk DNA was extracted from soil aggregates under $H_2{}^{18}O$ and $H_2{}^{16}O$ treatments.
181 DNA was centrifuged by density gradients and modified on a small scale as described
182 by Liu et al. (2019b). DNA was mixed with gradient buffer CsCl solution in Beckman
183 ultra-centrifuge tubes. After centrifugation at 177,000 g(av) for 44 h at 20 °C in a
184 Vti65.2 vertical rotor (Beckman Coulter, Palo Alto, CA, USA), the DNA was divided
185 into 14 equal fractions (Zhang et al., 2019a). The isolated DNA was purified and
186 dissolved in TE buffer.

187 **2.4. Quantitative PCR and sequencing processes**

188 To measure the growth and efficiency of ^{18}O incorporation into the bacterial
189 community genomic DNA, quantitative PCR (qPCR) was performed on a
190 LightCycler® 480II (Roche, Germany) for each buoyant density of DNA gradient
191 fraction targeting 16S rRNA genes using the primer pair 515F and 806R (Walters et al.,
192 2016). The amplification efficiencies of all genes ranged from 89 to 105%, and R values
193 ranged from 0.992 to 0.999.

194 Bacterial 16S rRNA genes were amplified in bulk DNA and in DNA gradient
195 fractions for each buoyant density from soil aggregates with $H_2{}^{18}O$ treatments using
196 primer pair 515F and 806R with 12bp barcodes (Walters et al., 2016). Sequence
197 libraries were generated using NEBNext® Ultra™ DNA Library Prep Kit for
198 Illumina® (New England Biolabs, MA, USA) according to the manufacturer's

199 recommendations. The libraries were sequenced on an Illumina HiSeq 2500 Platform
200 (Illumina, San Diego, CA, USA) by Guangdong Magigene Biotechnology Co. Ltd.
201 (Guangzhou, China).

202 Raw fastq files were quality-filtered using Trimmomatic and merged using FLASH
203 as described previously (Liu et al., 2020b). Operational taxonomic units (OTUs) were
204 clustered using UPARSE (version 10 http://drive5.com/uparse/) with a similarity cutoff
205 of 97%. In total we obtained 15,819,045 high-quality 16S rRNA sequences (92 samples
206 with average 171,946 reads per sample), which were clustered into 26803 OTUs. To
207 avoid potential bias caused by sequencing depth, all sequence data were rarefied to
208 121317 and 91425 sequences per samples in active and total bacteria for the diversity
209 analysis, respectively. The most frequently occurring sequences were extracted as
210 representative sequences for each OTU and the Silva (https://www.arb-silva.de/)
211 database was used to filter taxonomic annotations. The sequencing reads of the 16S
212 rRNA genes were stored in the Genome Sequence Archive (GSA, China) database with
213 the accession number CRA005780.

214 **2.5. Statistical analysis**

215 All data analysis was performed in the R environment (v3.6.3; http://www.r-
216 project.org) (Hamilton and Ferry, 2018).

217 To identify OTUs associated with ^{18}O assimilation, the R package DESeq2 was
218 used. The abundance of differential genes with negative binomial distributions in high-
219 density gradient (heavy) fractions based on $H_2{}^{18}O$ labelled treatments relative to
220 corresponding gradient fractions of non-labelled control [^{16}O] was carried out (Love et

al., 2014; Kong et al., 2019). Log2-fold changes above zero with padj value (FDR-adjusted P-value) of less than 10% were selected as ^{18}O labelled OTUs. Scatter plots were performed to visualize differentially labelled OTUs in heavy DNA fractions using the plotMA function.

Diversity indexes such as Shannon, Simpson and Richness were estimated using the vegan package (Dixon, 2003). The differences of beta diversity were calculated by Principal coordinate analysis (PCoA) with the Bray-Curtis distance of bacterial community profiles using vegan and ggplot2 packages (Lozupone et al., 2011), and two-way permutational multivariate analysis of variance (PERMANOVA) was used to quantitatively measure the effects of the incubation time and aggregate treatment.

OTUs were also used to evaluate the main species phylum among aggregates and time of incubation, and to calculate the relative abundance of the top ten abundant phylum by using amplicon and reshape2 packages. To ascertain the changes of interactions between bacterial groups as the incubation days and soil aggregates changed, co-occurrence networks among bacteria were described using the igraph package and the Gephi 0.9.2 platform (Bastian et al., 2009; Chen et al., 2020). Setting the filtering threshold of spearman correlation coefficients >0.6 and p-values <0.05, the significance of edges between nodes were determined. Prior to network analysis, excess OTUs were removed when they were present in less than ~90% of samples or when their relative abundance was less than 0.01% (Liu et al., 2022b). The network was further used to calculate topology property parameters. According to the nodes and links in the network, the main phylum in the network were determined.

To assess the assembly processes of bacteria in days with different aggregates and to assess responses to environmental factors, we used the normalized stochastic ratio (NST), which evaluates the underlying mechanisms of bacterial community assembly (Ning et al., 2019). NST was assessed based on cao, mGower, gower and binomial distance metrics in same null model algorithms [with 50% as the boundary, more stochastic (>50%) or more deterministic (<50%)], which is suggested to estimate the stochastic effects in community assembly (Ning et al., 2019). Statistically significant differences in alpha diversity indices, NST indices among incubation days and soil aggregates were determined by two-way analysis of variance (ANOVA), accompanied with least significant difference (LSD) test for multiple comparisons. Moreover, if the observed variances were heterogeneous, the group variance was calculated by a nonparametric Kruskal-Wallis test.

To compare different functional profiles in different incubation days and soil aggregates, we used Tax4Fun, which predicts functional profiles of the bacterial community from 16S rRNA gene sequences (Wemheuer et al, 2020; Ahauer et al, 2015). Data were then compared with KEGG (Kyoto Encyclopedia of Genes and Genomes) functional database at level 2, and the biological metabolic pathways could be significantly identified. After calculating the relative abundance of each functional profile, we used analysis of variance (ANOVA) as well as by LSD test for multiple comparisons among soil aggregates and days for functional profiles, printing those that were significantly different among incubation days and soil aggregates ($p<0.05$). By using Z scores, we printed functional profiles in the Tidyverse and reshape2 packages.

265 Correlation analysis among main species phylum in network and functional profiles of
266 ^{18}O labelled soil were performed by using Z scores based on Pearson correlations.
267
268 **3. Results**
269 **3.1. Labelling of active bacteria with $H_2{}^{18}O$**
270 On days 2 and 4, DNA obtained from $H_2{}^{16}O$ and $H_2{}^{18}O$ microcosms was separated
271 by isopycnic ultra-centrifugation to isolate ^{18}O-labelled DNA (heavy fractions) from
272 unlabelled DNA (light fractions). Compared to that of $H_2{}^{16}O$ control microcosms, 16S
273 rRNA buoyant density in the $H_2{}^{18}O$ treatment showed a relative shift to higher buoyant
274 densities, with detection of ^{18}O-DNA at buoyant density of 1.723-1.744 g ml^{-1} (the 6th
275 – 8th fractions), irrespective of the incubation time (Fig. 1). Thus, the 6th, 7th and 8th
276 fractions were individually selected as representatives of heavy DNA fractions (^{18}O-
277 DNA) for 16S rRNA gene sequencing.
278 **3.2. Diversity and taxonomic composition of active bacteria in soil aggregates**
279 For alpha diversity, Shannon and Simpson indexes of total bacteria showed
280 significant differences across aggregate fractions ($p < 0.001$in both tests) or incubation
281 time ($p = 0.029$, $p = 0.003$), while not for integrated effects of aggregates and incubation
282 time ($p = 0.473$, $p = 0.144$) (Fig. 2a, c). Shannon and Simpson diversity of active
283 bacteria also differed among aggregate fractions ($p = 0.016$, $p = 0.008$) (Fig. 2b, d). For
284 example, Shannon and Simpson indexes of SMA were shown to be separated from other
285 aggregates in active bacteria, especially for day 2. Compared to total bacteria, aggregate
286 fractions and incubation days showed clear synergies on Shannon and Simpson indexes

287 of active bacteria (p = 0.038, p = 0.014). Richness index of total bacteria also differed
288 by incubation days (p = 0.001) (Fig. S2). The Simpson index of active bacteria showed
289 significant differences (p = 0.001) between incubation time while no significant
290 difference (p = 0.139) was observed for Shannon indices (Fig. 2).

291 In terms of beta diversity, 49.56% of the variation in total bacterial community and
292 80.62% of variation in the active bacteria were explained by the first two axes of the
293 PCoA (Fig. 2e, f). In the total bacterial community, two-way PERMANOVA indicated
294 that incubation time explained 44.15% of variation in bacterial community while
295 aggregates only explained ~9.04% (Fig. 2e). We note that aggregates explained 19.56%
296 variation of active bacterial community, which is similar to the extent of incubation
297 time (26.42%) (Fig. 2f).

298 Taxonomic composition of total and labelled bacteria was calculated on the basis
299 of OTUs. The community of total bacteria was dominated by Proteobacteria (38.41%),
300 Chloroflexi (14.99%), and Acidobacteria (9.45%), while the labelled bacterial
301 community was dominated by Proteobacteria (54.80%) and Actinobacteria (28.57%)
302 (Fig. 3, Fig. S3). The relative abundance of Proteobacteria (54.80%) and Actinobacteria
303 (28.57%) increased in active bacterial communities compared to those in the total
304 communities (38.41% and 5.81%, respectively) (Fig. 3, Fig. S3). Additionally, all the
305 active bacterial OTUs were also detected in the total bacterial community. The ratio of
306 the number of active bacteria to total bacterial OTUs was 18.71%. The relative
307 abundance of reads of active bacterial OTUs in the total community was 91%. The
308 variation of bacterial composition was larger along with the soil aggregates and

309 incubation time in active bacterial community than that of total community (Fig. 3, Fig.
310 S3). The relative abundance of Proteobacteria and Actinobacteria in active bacteria
311 increased 1.2 fold (49.70% at day 2 to 60.03% at day 4) and decreased by one-third
312 (33.05% at day 2 to 22.21% at day 4) with incubation time, while those in total bacteria
313 decreased slightly for both Proteobacteria (39.32% at day 2 to 37.84% at day 4) and
314 Actinobacteria (5.83% at day 2 to 5.79% at day 4). The relative abundances of active
315 Proteobacteria and Actinobacteria in SMA (77.4%) were lower than that of MA
316 (86.32%%) and LMA (86.61%%) in active bacteria, while those were higher in SMA
317 (48.02%) compared to that in MA (42.72%) and LMA (42.41%) in total bacteria (Fig.
318 3b, S3b).

319 **3.3. The network and assembly processes of active bacteria in soil aggregates**

320 The network of bacteria at the phylum level between total and active bacterial
321 communities were different (Fig. 4). More OTUs were clustered in the networks of
322 active bacteria than the total bacterial communities at the phylum level (Fig. 4). The
323 total number of nodes, the number of links, the average degree and the modularity of
324 the active bacterial community were higher than the total bacterial community (Table
325 S2). In the active bacterial community, there were more negative correlations compared
326 to that of the total bacterial community (Table. S2). Together, networks of the labelled
327 community showed more links and higher network complexity than that in the total
328 community.

329 The NST explained the changes in ecological community assembly processes
330 based on incubation time and aggregate scales (Fig. 5). In the total bacterial community,

331 the value was less than 50%, suggesting that deterministic processes dominated
332 bacterial community assembly. Incubation days significantly influenced ecological
333 community assembly processes in the total bacterial community ($p < 0.05$) (Fig. 5a, c;
334 Fig. S4c). However, aggregates showed more significant effects on ecological
335 community assembly processes of the active bacterial community ($p < 0.05$) than
336 incubation time (Fig. 5b, d; Fig. S3d). For instance, NST of SMA was different from
337 NST of MA and LMA in the active bacterial community. Especially at day 2, the
338 ecological community assembly processes of SMA in the active bacterial community
339 was dominated by stochastic processes. Synergies between days and aggregates
340 influenced the ecological community assembly processes in active bacterial community
341 ($p < 0.05$) (Fig. 5b, d).

342 **3.4. Predictive functional profiles of active bacteria**

343 The prediction map showed the results with significant differences among
344 aggregates ($p < 0.05$). Predicted KEGG pathways at level 1 for both total (73.22%) and
345 active bacteria (61.87%) among aggregates were dominated by metabolism. However,
346 compared to total bacteria, functional profiles in active bacteria were significantly
347 different among aggregates (Fig. 6).

348 Among active bacteria, the functional profiles of the labelled soil bacterial
349 community on day 4 changed significantly compared to day 2 ($p < 0.05$) (Fig. S5).
350 Functional profiles related to metabolism decreased (62.22% to 61.52%), except for
351 amino acid metabolism. However, the relative abundance of other important functional
352 profiles increased, such as cell motility and signal transduction (Fig. S5). For aggregates,

353 the function of SMA differed from MA and LMA, in which amino acid metabolism,
354 cell motility, cell growth and death, and bacterial infectious disease were the key
355 functions (Fig. 6b). Correlations between major taxa and functional genes also differed
356 in SMA and other aggregates (Fig. S6).
357
358 **4. Discussion**
359 **4.1. Active and total bacteria identified using ^{18}O-SIP**
360 In this study, compared to total bacterial community, the composition, network
361 interactions, assembly processes and functional profiles in the active bacterial
362 community were different (Fig. 3, Fig. 4, Fig. 5, Fig. 6). We found that the relative
363 abundances of active bacterial reads occupied 91% of the total community, though the
364 number of OTUs in active communities occupied only 18.71% of the total communities.
365 This was consistent with previous studies in so much that the most abundant 4% of
366 OTUs represented a high relative abundance (54%) of reads, and most bacteria in soils
367 are found to be metabolically active when incubated with $H_2{}^{18}O$ (Lundberg et al., 2012;
368 Papp et al., 2018a, 2018b). This indicates that most bacterial taxa in soil are able to
369 respond rapidly and are active when conditions are favourable (Mueller et al., 2016).
370 The results of this study are similar to that of a previous study in which ^{18}O-labelled
371 bacteria community showed different patterns and more significant random
372 phylogenetic distribution compared to total bacteria (Coskun et al., 2019). Certain phyla
373 represented a greater proportion of active bacteria, in particular Proteobacteria (38.58%
374 in total bacteria to 55.32% in active bacteria) and Actinobacteria (5.81% in total bacteria

375 to 28.12% in active bacteria) (Fig. 3, Fig. S3). The dominance of Proteobacteria and
376 Actinobacteria among paddy soil active bacteria has been reported previously (Wu et
377 al., 2011; Itoh et al., 2013). Wisnoski et al. (2020) speculated that potential habitat
378 generalists, including Proteobacteria and Actinobacteria, with wide niche breadths can
379 adapt to flooded conditions. The habitat preference of soil bacterial families is closely
380 related to their respiratory characteristics, and these results are also attributed to
381 respiratory characteristics of different bacteria (Shen et al., 2021). Many Proteobacteria
382 were likely enriched under flooding due to their capacity for anaerobic respiration (Dai
383 et al., 2021; Wang et al., 2012).

384 Network analysis showed that there were more nodes, OTU links, average degree,
385 and modularity in the active bacterial community compared to the total bacterial
386 community (Fig. 4, Table S2), indicating more intensive interactions among active
387 bacteria. Positive links dominated in all networks, indicating that microbial synergy
388 plays an important role (Zhou et al, 2020). However, the proportion of negative
389 correlations of active bacteria was nearly twice (28.02%) that of the total bacterial
390 community (14.83%). As the negative links among nodes could be attributed to
391 competition, amensalism and opposing niche preferences among microbes, these
392 results suggest stronger competitive interaction or opposite niche preference among the
393 active Proteobacteria and Actinobacteria (Dai et al., 2021; Faust and Raes, 2012; Wang
394 et al., 2021). Additionally, assembly processes of the total bacterial community in paddy
395 fields were dominated by deterministic processes (Fig. 5). Deterministic processes of
396 abundant taxa have also been found in paddy soils (Hou et al., 2020). It is suggested

that soil pH and organic matter are deterministic factors that drive assembly processes of bacterial communities (Dini Andreote et al., 2015; Tripathi et al., 2018). Higher soil pH (>6.7) also leads to deterministic assembly of abundant populations (Jiao and Lu, 2020). In this study, deterministic processes of total bacteria might be attributed to the neutral pH (6.9 ± 0.08) and low soil organic matter (13.5 ± 0.01 g kg^{-1}) of bulk soil. Interestingly, stochasticity was more important in governing soil active microbes than the total bacteria (Fig. 5). Flooding conditions promoted by hydrologic mixing presumably enhanced the ability of active microorganisms to migrate across geographical areas, which might explain why the stochastic processes in active bacteria were more important than in total bacteria (Liu et al., 2020a; Liu et al., 2022a). Besides, we found the stochastic processes increased with decreasing bacterial richness from total bacteria to labelled bacteria (Fig. S2). This result may be attributed to stochastic assembly processes inducing synergy among microorganisms (Jiao et al., 2020), which might lead to greater competition with species richness reduction (Grime, 1973; Rajaniemi, 2002).

For functional profiles, predicted KEGG pathways at level 1 for both total (73.22%) and active bacteria (61.87%) were dominated by metabolism, and the relative abundance of other functions, such as environmental information processing, in active bacteria (19.39%) increased compared to that of total bacteria (11.22%) (Fig. 6). Similar results have also confirmed that metabolic genes are dominant in anoxic environments (Lesniewski et al., 2012), and other studies have revealed that members of the phylum Proteobacteria are key drivers of the important metabolic activities in soil ecosystems

(Salam and Obayori, 2019). Previious studies have shown that the active community is more closely related to functional profiles than the total community (e.g., Bastida et al., 2016). In summary, higher proportion of Proteobacteria and Actinobacteria, more negative correlations, more stochasticity in assembly processes and more different functional profiles were observed in ^{18}O-labelled bacteria compared to total bacteria.

4.2. Succession of active microbes and functional profiles along with incubation time

Previous studies have shown succession of bacterial communities in paddy fields, for instance, Ding et al. (2017) showed succession of diversity and functional profiles of active bacteria with incubation time. Furthermore, Yang et al. (2019b) found that bacterial diversity was higher in flooded areas than in control areas, whereas other studies found that soil bacterial diversity was lower in water-saturated soil (Zhou et al., 2002; Kozdrój and van Elsas, 2000). In our study, the diversity increased from day 2 to day 4 in active bacteria (Fig. 2). It is found that some bacteria that can survive periods of hypoxia could revive from inactive states and thrive under flooded conditions (Berney et al., 2014; Furtak et al., 2020; Fredrickson et al., 2008). Furthermore, flooded environments promote active bacterial colonization in soil, and bacteria actively use alternative electron acceptors for respiration to manage hypoxia (Eggleston et al., 2015; Engelhardt et al., 2018; Yan et al., 2015). Similar to species diversity, the composition of active bacteria also differed with incubation time (Fig. 3b, Fig. S3b). It is known that flooded conditions can increase abundance of some populations, such as Proteobacteria, and Bacteroidetes (Afzal et al., 2019; de León-Lorenzana et al., 2017; Zhang et al.,

2019b). In our study, the relative abundance of Actinobacteria decreased from day 2 (33.9%) to day 4 (22.34%), while Proteobacteria increased from day 2 (50.7%) to day 4 (59.95%) (Fig. 3). The variation of Actinobacteria and Proteobacteria in active bacteria might be due to different reproductive strategies. Actinobacteria are ubiquitous and usually predominant in arid habitats. Their drought tolerance may stem from their unique life-cycle characteristics (Lebre et al., 2017), including mycelial growth (Jones and Elliot, 2017) and arthrospore formation (Kämpfer et al., 2014). In contrast, Proteobacteria are more adapted to flooded conditions and more competitive under such circumstances, and a similar trend has been observed in wet soil compared to dry soil (Na et al., 2019). Additionally, the relative abundance of Gemmatimonadetes increased from 2.63% in day 2 to 4.11% in day 4 (Fig. 3b, Fig. S3b). Growth of Gemmatimonadetes could be attributed to their ability to survive low-oxygen conditions (Debruyn et al., 2011).

As for the predicted genes of active microbes, after 4 days of incubation, the functional profiles changed significantly compared to that in day 2 (Fig. S5). Functional profiles related to metabolism still dominated even though it decreased from 62.22% at day 2 to 61.52% at day 4. For metabolism, amino acid metabolism increased, while others, such as carbohydrate metabolism decreased (Fig. S5). Salam (2019) found that amino acid metabolism is mainly predicted by Proteobacteria. More amino acid metabolism functional genes were found with incubation, which is paralleled by the increase in relative abundance of Proteobacteria (Fig. S3b; Fig.S5). For carbohydrate metabolism, these results can be attributed to the submergence condition, which

463 decreases carbohydrate metabolism of bacteria in soil (Moreno-Espindola et al., 2018;
464 Ding et al., 2019). Lower metabolism function was predicted at day 4 compared to day
465 2, which could be due to the decrease of Actinobacteria, as Actinobacteria are reported
466 to contribute to the production of secondary metabolites (Yan et al., 2021) (Fig. S3b).
467 Furthermore, some studies showed that flooding increases nutrient availability in soil
468 (Oorschot et al., 2000; Shekiffu and Semoka, 2007). Qiu et al. (2020) found that the
469 addition of organic matter activates connections and closes relationships among
470 microorganisms as incubation progresses. We assume that flooded soils have similar
471 influences on the active bacterial community, making more nutrients available, hence
472 the predicted abundance of genes in many KEGG pathways increased, including
473 environmental information processing, cellular processes, organismal systems and
474 human diseases. For example, the predicted abundance of genes involved in cell
475 motility and signal transduction for the active bacteria showed a significant increase at
476 day 4 compared to day 2 (Fig. S5). The relative abundance of active Bacteroidetes
477 nearly doubled from 1.49% in day 2 to 2.84% at day 4 (Fig. 3b, Fig. S3b). Bacteroidetes
478 are highly effective at secreting carbohydrate-active enzymes and immobilizing them
479 to cell surfaces, and may increase cell motility across solid surfaces (Larsbrink and
480 Mckee, 2020). Signal transduction of soil microbiomes is promoted by environmental
481 stresses (Sun et al., 2020), which is consistent with incubations at day 4 showing a
482 higher relative abundance of signal transduction compared to day 2. In brief, as
483 diversity of active bacteria increased, composition became more complex from day 2
484 to day 4, and the relative abundance of many functional profiles also increased. A large

proportion of functional gene species can be altered due to changes in biodiversity and composition (Jung et al, 2016).

4.3. Diversity, assembly processes and functional profiles of active bacteria across aggregates

Some researchers have found that the bacterial communities among different aggregates are indeed different (Bailey et al., 2013; Trivedi et al.,2017). Especially for active bacteria, it was shown that there were more differences between aggregates compared to total bacteria (Fig. 2; 4). Bacteria diversity tends to increase with increasing aggregate size (Lupwayi et al., 2001), while bacterial biomass and diversity are higher in small aggregates with more stable structure (Hernández and López-Hernández, 2002; Ling et al., 2014). In our study, the diversity of active bacteria in SMA was higher than MA and LMA, and nearly all active bacteria were more enriched in SMA compared to MA and LMA (Fig. 2, Fig. 3). A possible interpretation of this finding is that SMA provides more nutrients compared to MA and LMA (Wang et al., 2014; Ling et al., 2014). It is found that soil organic matter and total nitrogen increase as aggregates become larger (from MA to SMA) (Lin et al., 2019; Zheng et al., 2021). LMA is poor in nutrients, while SMA shows the opposite (Tang et al., 2022; Zhang et al., 2021). In addition, the diversity of active bacteria is also correlated with soil porosity (Yang et al., 2019a). The higher diversity in SMA compared to MA might also be attributed to the higher soil porosity in SMA. While nutrient contents of aggregates lead to differences in bacteria diversity, it also has crucial effects on assembly processes. Liao et al. (2022) found that bacterial assembly processes in macro- and micro-

aggregates are mainly affected by total carbon and soil organic carbon. Better nutrient availability in SMA compared to MA and LMA may make stochastic processes dominate the assembly (Fig. 4) (Lin et al., 2019; Tang et al., 2022; Zheng et al., 2021). In our study, we found that active bacteria in SMA are dominated by stochasticity, while active bacteria in other aggregates showed more deterministic processes (Fig. 4). Our study is consistent with previous reports showing that environments with restrictive nutrients are dominated by deterministic processes, while the stochastic processes are more prevalent in environments with greater nutrient availability (Chase, 2010; Wang et al., 2015). In addition to nutrients, biological interactions may also contribute to a strong environmental filtering in MA and LMA (Vos et al., 2013; Jiang et al., 2017). Compared to SMA, the networks of MA and LMA had a higher complexity and a larger proportion of links (Fig.3, Table. S2). The more intense microbial interactions in MA and LMA indicated stronger environmental filtering with more deterministic processes compared to SMA (Fan et al., 2018; Liao et al., 2020). It is also worth noting that nutrients and structure of aggregates were not measured in this study as the amount of soil obtained was insufficient after aggregate fractionation. Moreover, additional measurements of other soil physicochemical properties and nutrient levels should be included in future studies to determine biological feedback mechanisms under different physicochemical properties and nutrient levels.

Differentiated communities in aggregates among active bacteria suggest different community functions. The functional prediction map showed that function associated with SMA differed from MA and LMA. Amino acid metabolism, cell motility, cell

growth and death, and bacterial infectious disease were key functions found in ^{18}O-labelled SMA (Fig. 6b). Functional profiles of amino acid metabolism in SMA showed a relatively high abundance compared to those in MA and LMA, in which Proteobacteria dominated (Salam and Obayori, 2019). This study also showed a significant positive correlation of Proteobacteria in SMA to amino acid metabolism than that in MA and LMA (Fig. S6). As the most abundant phylum (Fig. 3; Fig. S3), Proteobacteria likely determined cell motility genes by means of flagella movement in active bacteria (Anderson et al., 2010; Beeby, 2015). Compared to that in MA (58.99%) and LMA (59.61%), the relative abundance of Proteobacteria in SMA (61.25%) was higher at day 4 (Fig. 3, Fig. S3). Hence the relative abundance of cell motility genes is higher in SMA compared to MA and LMA. For cell growth and death, SMA provides more nutrients compared to MA and LMA (Lin et al., 2019; Tang et al., 2022; Zhang et al., 2021). This is consistent with higher relative abundance of cell growth and death genes in SMA compared to MA and LMA. Proteobacteria also contribute to bacterial infectious diseases, for example, *Salmonella* and *Vibrio* of Proteobacteria include pathogenic species. Besides, symbiotic relationships between Gammaproteobacteria and invertebrates like nematodes have been found (Williams et al., 2010), suggesting their interaction with potential parasites, thus explaining the relatively high abundance of bacterial infectious disease functions in SMA compared with MA and/or LMA. Together, the diversity and composition of active bacteria in SMA is more complex, assembly processes in SMA are more deterministic, and higher relative abundance of key functional profiles are predicted compared with MA and LMA.

5. Conclusion

We applied $H_2{}^{18}O$ based DNA-SIP to identify active bacterial community in paddy soil aggregates and showed that higher microbial diversity, different composition, more complex networks and more stochastic processes were associated with active bacteria compared to the total bacterial community. The active bacterial community and their predicted functional profiles changed significantly with the incubation time and soil aggregate sizes. Compared to other soil aggregates where deterministic processes dominated, the assembly processes of active bacteria in SMA were dominated by stochastic forces probably due to the richer nutrient status. In summary, this research improves our understanding of active bacterial communities and their assembly processes among soil aggregates in paddy fields.

Acknowledgements

This research was financially supported by the National Key Research and Development Program of China (2021YFD1900300) and National Natural Science Foundation of China (41977033, 41721001).

References

Aanderud, Z.T., Lennon, J.T., 2011. Validation of heavy-water stable isotope probing for the characterization of rapidly responding soil bacteria. Applied and environmental microbiology 77 (13), 4589-4596.

Ahauer, K.P., Wemheuer, B., Daniel, R., Meincke, P., 2015. Tax4fun: predicting

573 functional profiles from metagenomic 16S rRNA data. Bioinformatics 31 (17),
574 2882-2884.
575 Afzal, M., Yu, M.J., Tang, C.X., Zhang, L.J., Muhammad, N., Zhao, H.C., Feng, J.Y.,
576 Yu, L., Xu, J.M., 2019. The negative impact of cadmium on nitrogen
577 transformation processes in a paddy soil is greater under non-flooding than
578 flooding conditions. Environment international 129, 451-460.
579 Anderson, J. K., Smith, T. G., Hoover, T. R., 2010. Sense and sensibility: flagellum-
580 mediated gene regulation. Trends in microbiology 18 (1), 30-37.
581 Bach, E.M., Williams, R.J., Hargreaves, S.K., Yang, F., Hofmockel, K.S., 2018.
582 Greatest soil microbial diversity found in micro-habitats. Soil Biology and
583 Biochemistry 118, 217-226.
584 Bahram, M., Hildebrand, F., Forslund, S.K., Anderson, J.L., Soudzilovskaia, N.A.,
585 Bodegom, P.M., Bengtsson-Palme, J., Anslan, S., Coelho, L.P., Harend, H.,
586 HuertaCepas, J., Medema, M.H., Maltz, M.R., Mundra, S., Olsson, P.A., Pent, M.,
587 Põlme, S., Sunagawa, S., Ryberg, M., Tedersoo, L., Bork,P., 2018. Structure and
588 function of the global topsoil microbiome. Nature 560 (7717), 233–237.
589 Bai, R., Wang, J.T., Deng, Y., He, J.Z., Feng, K., Zhang, L.M., 2017. Microbial
590 Community and Functional Structure Significantly Varied among Distinct Types
591 of Paddy Soils But Responded Differently along Gradients of Soil Depth Layers.
592 Frontiers in Microbiology 8, 945.
593 Bai, S., Li, J., He, Z., Van Nostrand, J. D., Tian, Y., Lin, G., Zhou, J., Zheng, T., 2013.
594 GeoChip-based analysis of the functional gene diversity and metabolic potential

595 of soil microbial communities of mangroves. Applied microbiology and
596 biotechnology 97 (15), 7035–7048.
597 Bailey, V.L., McCue, L.A., Fansler, S.J., Boyanov, M.I., DeCarlo, F., Kemner, K.M.,
598 Konopka, A., 2013. Micrometer-scale physical structure and microbial
599 composition of soil macroaggregates. Soil Biology and Biochemistry 65, 60–68.
600 Bardgett, R.D., Van Der Putten, W.H., 2014. Belowground biodiversity and ecosystem
601 functioning. Nature 515 (7528), 505–511.
602 Barq, M.G., Hassan, M.M., Yasmin, H., Shahzad, A., Malik, N.H., Lorenz, N., Alsahli,
603 A.A., Dick, R.P., Ali, N., 2021. Variation in archaeal and bacterial community
604 profiles and their functional metabolic predictions under the influence of pure and
605 mixed fertilizers in paddy soil. Saudi Journal of Biological Sciences 28 (11), 6077-
606 6085.
607 Bastian, M., Heymann, S., Jacomy M., 2009. Gephi: an open source software for
608 exploring and manipulating networks. Proceedings of the International AAAI
609 Conference on Web and Social Media 3 (1), 361–362.
610 Bastida, F., Torres, I.F., Moreno, J.L., Baldrian, P., Ondono, S., Ruiz-Navarro, A.,
611 Jehmlich, N., 2016. The active microbial diversity drives ecosystem
612 multifunctionality and is physiologically related to carbon availability in
613 Mediterranean semiarid soils. Molecular Ecology 25 (18), 4660–4673.
614 Beeby, M., 2015. Motility in the epsilon-proteobacteria. Current opinion in
615 microbiology 28, 115-121.
616 Berney, M., Greening, C., Conrad, R., Jacobs, W.R., Cook, G.M., 2014. An obligately

aerobic soil bacterium activates fermentative hydrogen production to survive reductive stress during hypoxia. Proceedings of the National Academy of Sciences of the United States of America 111 (31), 11479–1148.

Briar, S.S., Fonte, S.J., Park, I., Six, J., Scow, K., Ferris, H., 2011. The distribution of nematodes and soil microbial communities across soil aggregate fractions and farm management systems. Soil Biology and Biochemistry 43 (5), 905-914.

Chase, J.M., 2010. Stochastic community assembly causes higher biodiversity in more productive environments. Science 328 (5984), 1388–1391.

Chen, J., Wang, P.F., Wang, C., Wang, X., Miao, L.Z., Liu, S., Yuan, Q.S., Sun, S.H., 2020. Fungal community demonstrates stronger dispersal limitation and less network connectivity than bacterial community in sediments along a large river. Environmental Microbiology 22 (3), 832–849.

Coskun, Ö.K., Özen, V., Wankel, S.D., Orsi, W.D., 2019. Quantifying population-specific growth in benthic bacterial communities under low oxygen using $H_2{}^{18}O$. The ISME Journal 13 (6), 1546-1559.

Dai, Y.L., Pan, Y.S., Sun, Y., Zeng, J., Liu, G.M., Zhong, W.H., Li, X.Z., Wu, Y.C., Lin, X.G., 2021. Moisture effects on the active prokaryotic communities in a saline soil unraveled by ^{18}O-informed metagenomics. Journal of Soils and Sediments 21 (1), 430-440.

de León-Lorenzana, A. S., Delgado-Balbuena, L., Domínguez-Mendoza, C., Navarro-Noya, Y. E., Luna-Guido, M., Dendooven, L., 2017. Reducing salinity by flooding an extremely alkaline and saline soil changes the bacterial community but its effect

639 on the archaeal community is limited. Frontiers in Microbiology, 8, 466.
640 Debruyn, J.M., Nixon, L.T., Fawaz, M.N., Johnson, A.M., Radosevich, M.,2011.
641 Global Biogeography and Quantitative Seasonal Dynamics of Gemmatimonadetes
642 in Soil. Applied and environmental microbiology 77 (17), 6295-6300.
643 Del Giorgio, P.A., Gasol, J.M., 2008. Physiological Structure and Single-Cell Activity
644 in Marine Bacterioplankton. Microbial ecology of the oceans 2, 243-298.
645 Ding, L.J., Su, J.Q., Li, H., Zhu, Y.G., Cao, Z.H., 2017. Bacterial succession along a
646 long-term chronosequence of paddy soil in the Yangtze River Delta, China. Soil
647 Biology and Biochemistry 104, 59-67.
648 Ding, X.H., Luo, J., Li, Y.Z., Ren, B., Bian, H.L., Yao, X., Zhou, Q.Q., 2019. Survival
649 of completely submerged Salix triandroides cuttings is associated with non-
650 structural carbohydrate metabolism. Journal of Freshwater Ecology 34 (1), 395-
651 404.
652 Dini Andreote, F., Stegen, J.C., Elsas, J.V., Salles, J.F., 2015. Disentangling
653 mechanisms that mediate the balance between stochastic and deterministic
654 processes in microbial succession. Proceedings of the National Academy of
655 Sciences 112 (11), 1326-1332.
656 Dixon, P., 2003. VEGAN, a package of R functions for community ecology. Journal of
657 Vegetation Science 14 (6), 927–930.
658 Dong, M., Kowalchuk, G.A., Liu, H., Xiong, W., Deng, X., Zhang, N., Li, R., Shen, Q.,
659 Dini-Andreote, F., 2021. Microbial community assembly in soil aggregates: A
660 dynamic interplay of stochastic and deterministic processes. Applied Soil Ecology

163, 103911.

Dumont, M.G., Hernández, G.M., 2019. Stable isotope probing. Methods and Protocols Totowa, NJ, US: Humana Press.

Eggleston, E.M., Lee, D.Y., Owens, M.S., Cornwell, J.C., Crump, B.C., Hewson, I., 2015. Key respiratory genes elucidate bacterial community respiration in a seasonally anoxic estuary. Environment Microbiology 17 (7), 2306–2318.

Engelhardt, I.C., Welty, A., Blazewicz, S.J., Bru, D., Rouard, N., Breuil, M.C., Gessler, A., Galiano, L., Miranda, J.C., Spor, A., Barnard, R.L., 2018. Depth matters: effects of precipitation regime on soil microbial activity upon rewetting of a plant-soil system. The ISME Journal 12 (4), 1061–1071.

Fan, K., Weisenhorn, P, Gilbert, J.A., Chu, H., 2018. Wheat rhizosphere harbors a less complex and more stable microbial co-occurrence pattern than bulk soil. Soil Biology and Biochemistry 125, 251-260.

Faust, K., Raes, J., 2012. Microbial interactions: from networks to models. Nature Reviews. Microbiology 10 (8), 538-550.

Fierer, N., 2017. Embracing the unknown: disentangling the complexities of the soil microbiome. Nature Reviews Microbiology 15 (10, 579-590.

Fredrickson, J.K., Li, S.W., Gaidamakova, E.K., Matrosova, V.Y., Zhai, M., Sulloway, H.M., Daly, M.J., 2008. Protein oxidation: Key to bacterial desiccation resistance? The ISME Journal 2 (4), 393–403.

Furtak, K., Grzadziel, J., Galazka, A., Niedzwiecki, J., 2020. Prevalence of unclassified bacteria in the soil bacterial community from floodplain meadows (fluvisols)

683 under simulated flood conditions revealed by a metataxonomic approachss. Catena
684 188, 104448.
685 Grime, J.P., 1973. Competitive exclusion in herbaceous vegetation. Nature 242 (5396),
686 344-347.
687 Guo, J.H., Peng, Y.Z., Ni, B.J., Han, X.Y., Fan, L., Yuan, Z.G., 2008. Dissecting
688 microbial community structure and methane-producing pathways of a full-scale
689 anaerobic reactor digesting activated sludge from wastewater treatment by
690 metagenomic sequencing. Microbial Cell Factories 14 (1), 1-11.
691 Hamilton, N.E., Ferry, M., 2018. Ggtern: ternary diagrams using ggplot2. Journal of
692 Statistical Software 87, 1–17.
693 Han, S., Delgado-Baquerizo, M., Luo, X., Liu, Y., Van Nostrand, J.D., Chen, W., Zhou,
694 J., Huang, Q., 2021. Soil aggregate size-dependent relationships between
695 microbial functional diversity and multifunctionality. Soil Biology and
696 Biochemistry 154, 108143.
697 Helgason, B.L., Walley, F.L., Germida, J.J., 2010. No-till soil management increases
698 microbial biomass and alters community profiles in soil aggregates. Applied Soil
699 Ecology 46 (3),390–397.
700 Hemandez, R.M., López-Hernández, D., 2002. Microbial biomass, mineral nitrogen
701 and carbon content in savanna soil aggregates under conventional and no-tillage.
702 Soil Biology and Biochemistry 34 (11), 1563-1570.
703 Hou, J.Y., Wu, L.H., Liu, W.X., Ge, Y.Y., Mu, T.T., Zhou, T., Li, Z., Zhou, J.W., Sun,
704 X., Luo, Y.M., Christie, P., 2020. Biogeography and diversity patterns of abundant

and rare bacterial communities in rice paddy soils across China. Science of The Total Environment 730, 139116.

Hubbell, S.P., 2005. Neutral theory in community ecology and the hypothesis of functional equivalence. Functional ecology 19 (1), 166–172.

Huber, P., Metz, S., Unrein, F., Mayora, G., Sarmento, H., Devercelli, M., 2020. Environmental heterogeneity determines the ecological processes that govern bacterial metacommunity assembly in a floodplain river system. The ISME Journal 14 (12), 2951-2966.

Itoh, H., Ishii, S., Shiratori, Y., Oshima, K., Otsuka, S., Hattori, M., Senoo, K., 2013. Seasonal transition of active bacterial and archaeal communities in relation to water management in paddy soils. Microbes and Environments 28, 370-380.

Jiang, X., Wright, A.L., Wang, J., Li, Z., 2011. Long-term tillage effects on the distribution patterns of microbial biomass and activities within soil aggregates. Catena 87, 276-280.

Jiang, Y., Jin, C., Sun, B., 2014. Soil aggregate stratification of nematodes and ammonia oxidizers affects nitrification in an acid soil. Environmental Microbiology 16 (10), 3083-3094.

Jiang, Y., Sun, B., Jin, C., Wang, F., 2013.Soil aggregate stratification of nematodes and microbial communities affects the metabolic quotient in an acid soil. Soil Biology and Biochemistry 60,1–9.

Jiang, Y.J., Liu, M.Q., Zhang, J.B., Chen, Y., Chen, X.Y., Chen, X.Y., Chen, L.J., Li, H.X., Zhang, X.X., Sun, B., 2017. Nematode grazing promotes bacterial

727 community dynamics in soil at the aggregate level. The ISME Journal 11 (12),
728 2705-2717.
729 Jiao, S., Lu, Y.H., 2020. Soil pH and temperature regulate assembly processes of
730 abundant and rare bacterial communities in agricultural ecosystems.
731 Environmental Microbiology 22, 1052-1065.
732 Jiao, S., Yang, Y., Xu, Y., Zhang, J., Lu, Y., 2020. Balance between community
733 assembly processes mediates species coexistence in agricultural soil microbiomes
734 across eastern China. The ISME Journal 14 (1), 202-216.
735 Jiao, S., Zhang, B.G., Zhang, G.Z., Chen, W.M., Wei, G.H., 2021. Stochastic
736 community assembly decreases soil fungal richness in arid ecosystems. Molecular
737 Ecology 30 (17), 4338-4348.
738 Jones, S.E., Elliot, M.A., 2017. Streptomyces exploration: competition, volatile
739 communication and new bacterial behaviours. Trends in Microbiology 25 (7),
740 522–531.
741 Jones, S.E., Lennon, J.T., 2010. Dormancy contributes to the maintenance of microbial
742 diversity. Proceedings of the National Academy of Sciences 107 (13), 5881-5886.
743 Jung, J., Philippot, L., Park, W., 2016. Metagenomic and functional analyses of the
744 consequences of reduction of bacterial diversity on soil functions and
745 bioremediation in diesel-contaminated microcosms. Scientific Reports 6 (1), 1-10.
746 Kämpfer, P., Glaeser, S.P., Parkes, L., Van K.G., Dyson, P., 2014. The family
747 Streptomycetaceae. In: Rosenberg E, DeLong EF, Lory S, Stackebrandt E,
748 Thompson F (eds) The prokaryotes: Actinobacteria. Springer Berlin Heidelberg,

749 Berlin, pp889–1010.
750 Kandeler, E., Tscherko, D., Spiegel, H., 1999. Long-term monitoring of microbial
751 biomass, N mineralisation and enzyme activities of a Chernozem under different
752 tillage management. Biology and Fertility of Soils 28, 343–351.
753 Kong, Y.J., Ling, N., Xue, C., Chen, H., Ruan, Y., Guo, J.J., Zhu, C., Wang, M., Shen,
754 Q.R., Guo, S.W., 2019. Long-term fertilization regimes change soil nitrification
755 potential by impacting active autotrophic ammonia oxidizers and nitrite oxidizers
756 as assessed by DNA stable isotope probing. Environmental Microbiology 21 (4),
757 1224-1240.
758 Kozdrój, J., van Elsas, J.D., 2000. Response of the bacterial community to root exudates
759 in soil polluted with heavy metals assessed by molecular and cultural approaches.
760 Soil Biology and Biochemistry 32 (10), 1405-1417.
761 Kuramae, E.E., Yergeau, E., Wong, L.C., Pijl, A.S., Van Veen, J.A., Kowalchuk, G.A.,
762 2012. Soil characteristics more strongly influence soil bacterial communities than
763 land-use type. FEMS Microbiology Ecology 79 (1), 12-24.
764 Larsbrink, J., McKee, L. S., 2020. Bacteroidetes bacteria in the soil: Glycan acquisition,
765 enzyme secretion, and gliding motility. Advances in applied microbiology, 110,
766 63-98.
767 Laundberg, D.S., Lebeis, S.L., Paredes, S.H., Paredes, S.H., Yourstone, S., Gehring, J.,
768 Malfatti, S., Tremblay, J., Engelbrektson, A., Kunin, V., del Rio, T.G., Edgar, R.C.,
769 Eickhorst, T., Ley, R.E., Hugenholtz, P., Tringe, S.G., Dangl, J.L., 2012. Defining
770 the core Arabidopsis thaliana root microbiome. Nature 488, 86-90.

771 Lavelle, P., Decaens, T., Aubert, M., Barot, S., Blouim, M., Bureau, F., Margerie, P.,
772 Mora, P., Rossi, J.P., 2006. Soil invertebrates and ecosystem services. European
773 Journal of Soil Biology 42,3–15.
774 Lebre, P.H., De, M.P., Cowan, D.A., 2017.Xerotolerant bacteria: surviving through a
775 dry spell. Nature Reviews Microbiology 15 (5), 285–296.
776 Leff, B., Ramankutty, N., Foley, J.A., 2004. Geographic distribution of major crops
777 across the world. Global biogeochemical cycles 18 (1), 1–27.
778 Lesniewski, R.A., Jain, S., Anantharaman, K., Schloss, P.D., Dich, G.J., 2012. The
779 metatranscriptome of a deep-sea hydrothermal plume is dominated by water
780 column methanotrophs and lithotrophs. The ISME Journal 6 (12), 754-765.
781 Li, N., Yao, S.H., Qiao, Y.F., Zhou, W.X., You, M.Y., Han, X.Z., Zhang, B., 2015.
782 Separation of soil microbial community structure by aggregate size to a large
783 extent under agricultural practices during early pedogenesis of a Mollisol. Applied
784 Soil Ecology 88, 9–20.
785 Li, Y., Liu, H., Pan, H., Zhu, X., Liu, C., Zhang, Q., Luo, Y., Di, H., Xu, J., 2019. T4-
786 type viruses: Important impacts on shaping bacterial community along a
787 chronosequence of 2000-year old paddy soils. Soil Biology and Biochemistry 128,
788 89-99.
789 Li, Y.L., Wang, H., Tao, X.H., Wang, X.Z., Jin, W.Z., Gilbert, J.A., Zhu, Y.G., Zhang,
790 Z.J., 2021. Continental-Scale Paddy Soil Bacterial Community Structure,
791 Function, and Biotic Interaction. Msystems 6 (5), e01368-20.
792 Liao, H., Zhang, Y., Wang, K., Hao, X., Chen, W., Huang, Q., 2020. Complexity of

793 bacterial and fungal network increases with soil aggregate size in an agricultural
794 Inceptisol. Applied soil Ecology 154, 103640.
795 Liao, H., Hao, X.L., Zhang, Y.C., Qin, F., Xu, M., Cai, P., Chen, W.L., Huang, Q.Y.,
796 2022. Soil aggregate modulates microbial ecological adaptions and community
797 assemblies in agricultural soils. Soil Biology and Biochemistry 172, 108769.
798 Lin, Y.X., Ye, G.P., Kuzyakov, Y.K., Liu, D.Y., Fan, J.B., Ding., W.X., 2019. Long-term
799 manure application increases soil organic matter and aggregation, and alters
800 microbial community structure and keystone taxa. Soil Biology and Biochemistry
801 134, 187-196.
802 Ling, N., Sun, Y.M., Ma, J.H., Guo, J.J., Zhu, P., Peng, C., Yu, G.H., Ran, W., Guo,
803 S.W., Shen, Q.R., 2014. Response of the bacterial diversity and soil enzyme
804 activity in particle-size fractions of Mollisol after different fertilization in a long-
805 term experiment. Biology and Fertility of Soils 50 (6), 901-911.
806 Liu, D., An, S.S., Cheng, Y., Keiblinger, K., Huang, Y.M., 2014. Variability in Soil
807 Microbial Biomass and Diversity Among Different Aggregate-Size Fractions of
808 Different Land Use Types. Soil Science 179 (5), 242-249.
809 Liu, H., Ding, Y., Zhang, Q., Liu, X., Xu, J., Li, Y., Di, H., 2019a. Heterotrophic
810 nitrification and denitrification are the main sources of nitrous oxide in two paddy
811 soils. Plant and Soil 445 (1), 39–53.
812 Liu, H., Pan, H., Hu, H., Zhang, Q., Liu, Y., Jia, Z., Xu, J., Di, H., Li, Y., 2019b.
813 Archaeal nitrification is preferentially stimulated by rice callus mineralization in
814 a paddy soil. Plant and Soil 445 (1), 55–69.

Liu, W.J., Graham, E.B., Zhong, L.H., Zhang, J.W., Li, W.T., Li, Z.P., Lin, X.G., Feng, Y.Z., 2020a. Dynamic microbial assembly processes correspond to soil fertility in sustainable paddy agroecosystems. Functional Ecology, 34 (6),1244-1256.

Liu, M., Han, X., Tong, J., Zhu, H., Bai, X., 2020b. Mutual environmental drivers of the community composition, functional attributes and co-occurrence patterns of bacterioplankton in the composite aquatic ecosystem of Taihu watershed in China. FEMS Microbiology Ecology 96, 137.

Liu, W.J., Graham, E.B., Dong, Y., Zhong, L.H., Zhang, J.W., Qiu, C.W., Chen, R.R., Lin, X.G., Feng, Y.Z., 2021. Balanced stochastic versus deterministic assembly processes benefit diverse yet uneven ecosystem functions in representative agroecosystems. Environmental Microbiology 23 (1), 391-404.

Liu, X., Shi, Y., Teng, Y., Gao, G.F., Zhang, L.Y., Xu, R.Y., Li, C.X., Liu, R.Y., Liu, J.J., Chu, H.Y., 2022a. Distinct Co-occurrence Relationships and Assembly Processes of Active Methane-Oxidizing Bacterial Communities Between Paddy and Natural Wetlands of Northeast China. Frontiers in Microbiology 13, 809074.

Liu, Y., Ding, C., Xu, X., Wang, K., Li, Y., Pan, H., Zhang, Q., Dumont, M.G., Di, H.J., Xu, J.M., Li, Y., 2022b. Atmospheric methane oxidation is affected by grassland type and grazing and negatively correlated to total soil respiration in arid and semiarid grasslands in Inner Mongolia. Soil Biology and Biochemistry 173, 108787.

Love, M. I., Huber, W., Anders, S., 2014. Moderated estimation of fold change and dispersion for RNA-seq data with deseq2. Genome Biology 15 (12), 1-21.

837 Lozupone, C., Lladser, M.E., Knights, D., Stombaugh, J., Knight, R., 2011. UniFrac:
838 an effective distance metric for microbial community comparison. The ISME
839 Journal 5 (2), 169,–172.
840 Luna, G.M., Manini, E., Danovaro, R., 2002. Large fraction of dead and inactive
841 bacteria in coastal marine sediments: comparison of protocols for determination
842 and ecological significance. Applied and environmental microbiology 68(7),
843 3509-3513.
844 Lundberg, D.S., Lebeis, S.L., Paredes, S.H., Yourstone, S., Gehring, J., Malfatti, S.,
845 Tremblay, J., Engelbrektson, A., Kunin, V., del Rio, T.G., Edgar, R.C., Eichhorst,
846 T., Ley, R.E., Hugenholtz, P., Tringe, S.G., Dangl, J.L., 2012. Defining the core
847 Arabidopsis thaliana root microbiome. Nature 488, 86-90.
848 Lupwayi, N.Z., Arshad, M.A., Rice, W.A., Glayton, G.W., 2001. Bacterial diversity in
849 water-stable aggregates of soils under conventional and zero tillage management.
850 Applied Soil Ecology 16 (3), 251-261.
851 Moreno-Espíndola, I.P., Ferrara-Guerrero, M.J., Luna-Guido, M.L., Ramirez-
852 Villanueva, D.A., De Leon-Lorenzana, A.S., Gomez-Acata, S., Gonzalez- Terreros,
853 E., Ramirez-Barajas, B., Navarros-Noya, Y.E., Sanchez-Rodriguez, L.M.,
854 Fuentes-Ponce, M., Macedas-Jimenez, J.U., Dendoovem, L., 2018. The Bacterial
855 Community Structure and Microbial Activity in a Traditional Organic Milpa
856 Farming System Under Different Soil Moisture Conditions. Frontiers in
857 Microbiology 9, 27-37.
858 Mueller, R.C., Gallegos-Graves, L., Zak, D.R., Kuske, C.R., 2016. Assembly of Active

859 Bacterial and Fungal Communities Along a Natural Environmental Gradient.
860 Environmental Microbiology 71, 57-67.
861 Na, X., Yu, H., Wang, P., Zhu, W., Niu, Y., Huang, J., 2019. Vegetation biomass and soil
862 moisture coregulate bacterial community succession under altered precipitation
863 regimes in a desert steppe in northwestern China. Soil Biology and Biochemistry
864 136, 107520.
865 Ning, D.L., Deng, Y., Tiedje, J.M., Zhou, J.Z., 2019. A general framework for
866 quantitatively assessing ecological stochasticity. Proceedings of the National
867 Academy of Sciences of the United States of America 116 (34), 16892–16898.
868 Ofek-Lalzar, M., Sela, N., Goldman-Voronov, M., Green, S.J., Hadar, Y., Minz, D.,
869 2014. Niche and host-associated functional signatures of the root surface
870 microbiome. Nature Communications 5 (1), 1-9.
871 Ofiteru, I.D., Lunn, M., Curtis, T.P., Wells, G.F., Criddle, C.S., Francis, C.A., Sloan,
872 W.T., 2010. Combined niche and neutral effects in a microbial wastewater
873 treatment community. Proceedings of the National Academy of Sciences of the
874 United States of America 107 (35), 15345–15350.
875 Oorschot, M.V., Gaalen, N.V., Maltby, E., Mockler, N., Spink, A., Verhoeven, J.T.A.,
876 2000. Experimental manipulation of water levels in two French riverine grassland
877 soils. Acta Oecologica 21 (1), 49-62.
878 Pacchioni, R.G., Carvalho, F.M., Thompson, C.E., Faustino, A.L., Nicolini, F., Pereira,
879 T.S., Silva, R.C., Cantao, M.E., Garber, A., Vasconcelos, A.T., Agnez-Lima, L.F.,
880 2014. Taxonomic and functional profiles of soil samples fromAtlantic forest and

881 Caatinga biomes in northeastern Brazil. Microbiology 3 (3), 299-315.
882 Papp, K., Hungate, B.A., Schwartz, E., 2018a. Microbial rRNA Synthesis and Growth
883 Compared through Quantitative Stable Isotope Probing with $H_2{}^{18}O$. Applied and
884 environmental microbiology 84 (8), 2441-2417.
885 Papp, K., Mau R.L., Michaela, H., Benjamin, J.K., Bruce, A.H., Egbert, S., 2018b.
886 Quantitative stable isotope probing with $H_2{}^{18}O$ reveals that most bacterial taxa in
887 soil synthesize new ribosomal RNA. The ISME Journal 12 (12), 3043-3045.
888 Philippot, L., Raaijmakers, J.M., Lemanceau, P., Putten, W.H., 2013. Going back to the
889 roots: the microbial ecology of the rhizosphere. Nature Reviews Microbiology 11
890 (11), 789–799.
891 Qiu, G., Zhu, M., Contin, M., Nobili, M.D., Luo, Y., Xu, J.M., Brookes, P.C., 2020.
892 Evaluating the 'triggering response' in soils, using ^{13}C-glucose, and effects on
893 dynamics of microbial biomass. Soil Biology and Biochemistry 147, 107843.
894 Rajaniemi, T.K., 2002. Why does fertilization reduce plant species diversity? Testing
895 three competition--based hypotheses. Journal of Ecology, 90 (2), 316-324.
896 Roesch, L., Fulthorpe, R., Riva, A., Casella, G., Hadwin, A.K.M., Kent, A.D., Daroub,
897 S.H., Camargo, F.A., Farmerie, W.G., Triplett, E.W., 2007. Pyrosequencing
898 enumerates and contrasts soil microbial diversity. The ISME Journal 1 (4), 283–
899 290.
900 Salam, L.B., Obayori, O.S., 2019. Structural and functional metagenomic analyses of a
901 tropical agricultural soil. Spanish Journal of Soil Science 9 (1), 1-23.
902 Schwartz, E., 2007. Characterization of growing microorganisms in soil by stable

903 isotope probing with $H_2{}^{18}O$. Applied and environmental microbiology 73 (8),
904 2541-2546.
905 Schwartz, E., Van Horn, D.J., Buelow, H.N., Okie, J.G., Gooseff, M.N., Barrett, J.E.,
906 Takacs-Vesbach, C.D., 2014. Characterization of growing bacterial populations in
907 McMurdo Dry Valley soils through stable isotope probing with O-18-water. FEMS
908 Microbiology Ecology 89(2), 415-425.
909 Shekiffu, C.Y., Semoka, J.M.R., 2007. Evaluation of iron oxide impregnated filter paper
910 method as an index of phosphorus availability in paddy soils of Tanzania. Nutrient
911 Cycling in Agroecosystems 77 (2), 169-177.
912 Shen, R.C., Lan, Z.C., Rinklebe, J., Nie, M., Hu, Q.W., Yan, Z.F., Fang, C.M., Jin, B.S.,
913 Chen, J.K., 2021. Flooding variations affect soil bacterial communities at the
914 spatial and inter-annual scales. Science of The Total Environment 759, 143471.
915 Stegen, J.C., Lin, X.J., Fredrickson, J.K., Konopka, A.E., 2015. Estimating and
916 mapping ecological processes influencing microbial community assembly.
917 Frontiers in Microbiology 6, 370.
918 Stegen, J.C., Lin, X.J., Konopka, A.E., Fredrickson, J.K., 2012. Stochastic and
919 deterministic assembly processes in subsurface microbial communities. The ISME
920 Journal 6 (9), 1653–1664.
921 Sun, X., Zhang, L., Pei, J., Huang, L.F., 2020. Regulatory relationship between quality
922 variation and environment of Cistanche deserticola in three ecotypes based on soil
923 microbiome analysis. Scientific Reports 10 (1), 1-12.
924 Tang, S.R., Yuan, P., Tawaraya, K., Tokida, T., Fukuoka, M., Yoshimoto, M., Sakai, H.,

925 Hasegawa, T., Xu, K.K., Cheng, W.G., 2022. Winter nocturnal warming affects the
926 freeze-thaw frequency, soil aggregate distribution, and the contents and
927 decomposability of C and N in paddy fields. Science of The Total Environment
928 802, 149870.
929 Tripathi, B.M., Stegen, J.C., Kim, M., Dong, K., Adams, J.M., Lee, Y.K., 2018, Soil pH
930 mediates the balance between stochastic and deterministic assembly of bacteria.
931 The ISME Journal 12 (4), 1072-1083.
932 Trivedi, P., Delgado-Baquerizo, M., Jeffries, T.C., Trivedi, C., Anderson, I.C., Lai, K.,
933 McNee, M., Flower, K., PalSingh, B., Minkey, D., Singh, B.K., 2017. Soil
934 aggregation and associated microbial communities modify the impact of
935 agricultural management on carbon content. Environment Microbiology 19 (8),
936 3070–3086.
937 Vellend, M., Srivastava, D.S., Anderson, K.M., Brown, C.D., Jankowski, J.E.,
938 Kleynhans, E.J., Kraft, N.J.B., Letaw, A.D., Macdonald, A.A.M., Maclean, J.E.,
939 MyersSmith, I.H., Norris, A.R., Xue, X.X., 2014. Assessing the relative
940 importance of neutral stochasticity in ecological communities. Oikos 123 (12),
941 1420–1430.
942 Vos, M., Wolf, A.B., Jennings, S.J., Kowalchuk, G.A., 2013. Micro-scale determinants
943 of bacterial diversity in soil. FEMS Microbiology Reviews 37 (6), 936-954.
944 Walters, W., Hyde, E.R., Berg-Lyons, D., Ackermann, G., Humphrey, G., Parada, A.,
945 Gilbert, J.A., Jansson, J.K., Caporaso, J.G., Fuhrman, J.A., Apprill, A., Knight, R.,
946 2016. Improved bacterial 16s rRNA gene (v4 and v4-5) and fungal internal

947 transcribed spacer marker gene primers for microbial community surveys.
948 mSystems 1, e00009-15.
949 Wang, H., Guan, D.S., Zhang, R.D., Chen, Y.J., Hu. Y.T., Xiao, L., 2014. Soil
950 aggregates and organic carbon affected by the land use change from rice paddy to
951 vegetable field. Ecological Engineering 70, 206-211.
952 Wang, R., Dungait, J., Creamer, C., Cai, B., Li, B., Xu, Z., Zhang, Y., Ma, Y., Jiang, Y.,
953 2015. Carbon and Nitrogen Dynamics in Soil Aggregates under Long-Term
954 Nitrogen and Water Addition in a Temperate Steppe. Soil Science Society of
955 America Journal 79 (2), 527-535.
956 Wang, X., Lu, L., Zhou, X., Tang, X., Kuang, L., Chen, J., Shan, J., Lu, H., Qin, H.,
957 Adams, J., Wang, B., 2021. Niche Differentiation of Comammox Nitrospira in the
958 Mudflat and Reclaimed Agricultural Soils Along the North Branch of Yangtze
959 River Estuary. Frontiers in Microbiology 11, 618287.
960 Wang, Y., Sheng, H.F., He, Y., Wu, J.Y., Jiang, Y.X., Tam, N., Zhou, H.W., 2012.
961 Comparison of the Levels of Bacterial Diversity in Freshwater, Intertidal Wetland,
962 and Marine Sediments by Using Millions of Illumina Tags. Applied and
963 environmental microbiology 78 (23), 8264-8271.
964 Wemheuer, F., Taylor, J.A., Daniel, R., Johnston, E.L., Meinicke, P., Thomas, T.,
965 Wemheuer, B., 2020. Tax4fun2: prediction of habitat-specific functional profiles
966 and functional redundancy based on 16s rRNA gene sequences. Environmental
967 Microbiome 15 (1), 1.
968 Williams, K.P., Gillespie, J.J, Sobral, B.W.S., Nordberg, E.K., Snyder, E.E., Shallom,

969 J.M., Dickerman, A.W., 2010. Phylogeny of gammaproteobacteria. Journal of
970 Bacteriology 192, 2305-2314.
971 Wisnoski, N.I., Muscarella, M.E., Larsen, M.L., Peralta, A.L., Lennon, J.T., 2020.
972 Metabolic insight into bacterial community assembly across ecosystem boundaries.
973 Ecology 101 (4), e02968.
974 Wu, M., Qin, H., Chen, Z., Wu, J., Wei, W., 2011. Effect of long-term fertilization on
975 bacterial composition in rice paddy soil. Biology and Fertility of Soils 47 (4), 397-
976 405.
977 Yan, B.Y., Liu, N., Liu, M.H., Du, X.Y., Shang, F., Huang, Y., 2021. Soil actinobacteria
978 tend to have neutral interactions with other co-occurring microorganisms,
979 especially under oligotrophic conditions. Environmental Microbiology 23 (8),
980 4126-4140.
981 Yan, Q., Bi, Y., Deng, Y., He, Z., Wu, L., Van Nostrand, J.D., Shi, Z., Li, J.J., Wang, X.,
982 Hu, Z.Y., Yu, Y.H., Zhou, J.Z., 2015. Impacts of the Three Gorges Dam on
983 microbial structure and potential function. Scientific Reports 5 (1), 1-9.
984 Yan, Y.C., Wang, X., Guo, Z.J., Chen, J.Q., Xin, X.P., Xu, D.W., Yan, R.R., Chen, B.R.,
985 Xu, L.J., 2018. Influence of wind erosion on dry aggregate size distribution and
986 nutrients in three steppe soils in northern China. Catena 170, 159-168.
987 Yang, C., Chen, T., Yang, Y., Meyyappan, M., Lai, C., 2017. Enhanced acetone sensing
988 properties of monolayer graphene at room temperature by electrode spacing effect
989 and UV illumination. Sensors and Actuators B: Chemical 253, 77-84.
990 Yang, C., Liu, N., Zhang, Y., 2019a. Soil aggregates regulate the impact of soil bacterial

and fungal communities on soil respiration. Geoderma 377, 444-452.

Yang, F., Zhang, D.D., Wu, J.J., Chen, Q., Long, C.Y., Li, Y.H., Cheng, X.L., 2019b. Anti-seasonal submergence dominates the structure and composition of prokaryotic communities in the riparian zone of the Three Gorges Reservoir, China. Science of The Total Environment 663, 662-672.

Zhang, Q., Zhou, W., Liang, G., Sun, J., Wang, X., He, P., 2015. Distribution of soil nutrients, extracellular enzyme activities and microbial communities across particle-size fractions in a long term fertilizer experiment. Applied Soil Ecology 94, 59–71.

Zhang, Q., Li, Y., He, Y., Liu, H., Dumont, M.G., Brookes, P.C., Xu, J., 2019a. Nitrosospira cluster 3-like bacterial ammonia oxidizers and nitrospira-like nitrite oxidizers dominate nitrification activity in acidic terrace paddy soils. Soil Biology and Biochemistry 131, 229-237.

Zhang, Q., Chen, H., Huang, D., Xu, C., Zhu, H., Zhu, Q., 2019b. Water managements limit heavy metal accumulation in rice: Dual effects of iron-plaque formation and microbial communities. Science of The Total Environment 687, 790-799.

Zhang, S., Li, Q., Lü, Y., Zhang, X., Liang, W., 2013a. Contributions of soil biota to C sequestration varied with aggregate fractions under different tillage systems. Soil Biology and Biochemistry 62, 147–156.

Zhang, W. C., Gregory, A. S., Whalley, W. R., Ren, T. S., Gao, W.D., 2021. Characteristics of soil organic matter within an erosional landscape under agriculture in Northeast China: stock, source, and thermal stability. Soil and

1013 Tillage Research 209, 104927.
1014 Zhang, Y., Lu, Z., Liu, S., Yang, Y., He, Z., Ren, Z., Zhou, J., Li, D., 2013b. Geochip-
1015 based analysis of microbial communities in alpine meadow soils in the Qinghai-
1016 Tibetan plateau. BMC microbiology 13, 72.
1017 Zheng, W., Zhao, Z.Y., Lv, F.L., Wang, R.Z., Wang, Z.H., Zhao, Z.Y., Li, Z.Y., Zhai,
1018 B.N., 2021. Assembly of abundant and rare bacterial and fungal sub-communities
1019 in different soil aggregate sizes in an apple orchard treated with cover crop and
1020 fertilizer. Soil Biology and Biochemistry 156, 108222.
1021 Zhou, H., Gao, Y., Jia, X.H., Wang, M.M., Ding, J.J., Cheng, L., Bao, F., Wu, B., 2020.
1022 Network analysis reveals the strengthening of microbial interaction in biological
1023 soil crust development in the Mu Us Sandy Land, northwestern China. Soil
1024 Biology and Biochemistry 144, 107782.
1025 Zhou, J.Z., Ning, D.L., 2017. Stochastic community assembly: does it matter in
1026 microbial ecology? Microbiology and Molecular Biology Reviews 81 (4), e00002-
1027 17.
1028 Zhou, J., Xia, B., Treves, D.S., Wu, L.Y., Marsh, T.L., Oneill, R.V., Palumbo, A.V.,
1029 Tiedje, J.M., 2002. Spatial and resource factors influencing high microbial
1030 diversity in soil. Applied and Environment Microbiology 68 (1), 326-334.

1031 **Figure Legends**

1032 **Fig. 1**. The relative abundance of 16S rRNA genes in aggregates (MA, SMA, LMA)
1033 retrieved from the 100% maximum water-holding capacity of $H_2{}^{18}O$ and 100%
1034 maximum water-holding capacity of $H_2{}^{16}O$ treatments in the 2-day and 4-day
1035 DNA-SIP microcosms.

1036 **Fig. 2.** Diversity of Shannon (a, b), Simpson (c, d) index of total and ^{18}O labelled
1037 bacteria in the different aggregates and incubation days treatments. Different
1038 letters and asterisks indicate significant differences ($P < 0.05$) based on two-way
1039 analysis of variance (ANOVA) as well as by LSD test for multiple comparisons.
1040 Composition of principal coordinate analysis (PCoA) calculated based on Bray-
1041 Curtis distances. Each point of total bacteria (e) and labelled bacteria (f)
1042 corresponds to a different sample shaped by days and coloured by aggregates. The
1043 percentage of variation indicated in each axis corresponds to the fraction of the
1044 total variance explained by the projection. Two-way permutational multivariate
1045 analysis of variance (PERMANOVA) was employed to quantitatively assess the
1046 effects of the day and aggregate treatment. Single, double and three asterisks
1047 represent significance at $P < 0.05$, $P < 0.01$, and $P < 0.001$ respectively.

1048 **Fig. 3.** Relative abundance of the soil bacterial community composition in both (a) total
1049 bacteria and (b) active bacteria among days and aggregates.

1050 **Fig. 4.** Network analysis revealing the associations among 16S rRNA OTUs in (a) Total
1051 MA, (b) Total SMA, (c) Total LMA, (d) Labelled MA, (e) Labelled SMA, (f)
1052 Labelled LMA. Coloured nodes represent corresponding OTUs assigned to major

phylum. The size of nodes represents the number of links between the OTUs and others. Red and blue lines represent the positive and negative links between OTUs.

Fig. 5. Boxplot of (a) NST_{cao} and (c) NST_{mGower} values of total bacteria in nine treatments and boxplot of (b) NST_{cao} and (d) NST_{mGower} values of labelled bacteria in six treatments. Different letters and asterisks indicate significant differences ($P < 0.05$) based on two-way ANOVA test as well as by LSD test for multiple comparisons.

Fig. 6. The functional profiles are divided into day 2 and day 4 with significant differences showed by letters among aggregates (LSD test). The result of functional profiles that Z scores is showed in the heatmap. The relative abundance of function profiles and the significant differences are printed in the histogram. (a) The main functional differences in total bacteria are metabolism, cellular processes, organismal systems, human diseases and genetic information processing, (b) while in labelled bacteria are metabolism, environmental information processing, cellular processes, organismal systems and human diseases.

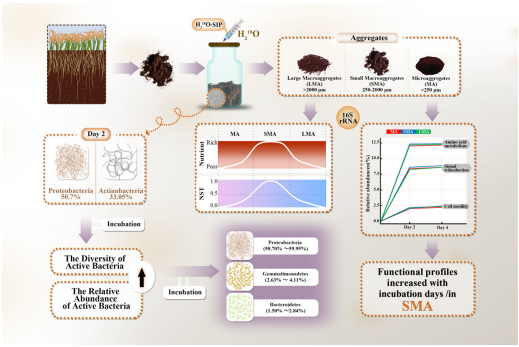
H2 18O-SIP
H2 18O
Aggregates
Large Macroaggregates (LMA) >2000 μm
Small Macroaggregates (SMA) 250-2000 μm
Microaggregates (MA) <250 μm
Day 2
Proteobacteria 50.7%
Actinobacteria 33.85%
MA
SMA
LMA
Nutrient
Pool
NST
1.0
0.5
0.0
16S rRNA
Amino acid metabolism
Signal transduction
Cell motility
Day 2
Day 4
Incubation
The Diversity of Active Bacteria
The Relative Abundance of Active Bacteria
Incubation
Proteobacteria (50.70% ~+16.93%)
Gemmatimonadetes (2.63% ~+4.11%)
Bacteroidetes (1.58% ~+2.64%)
Functional profiles increased with incubation days /in
SMA

Fig.1

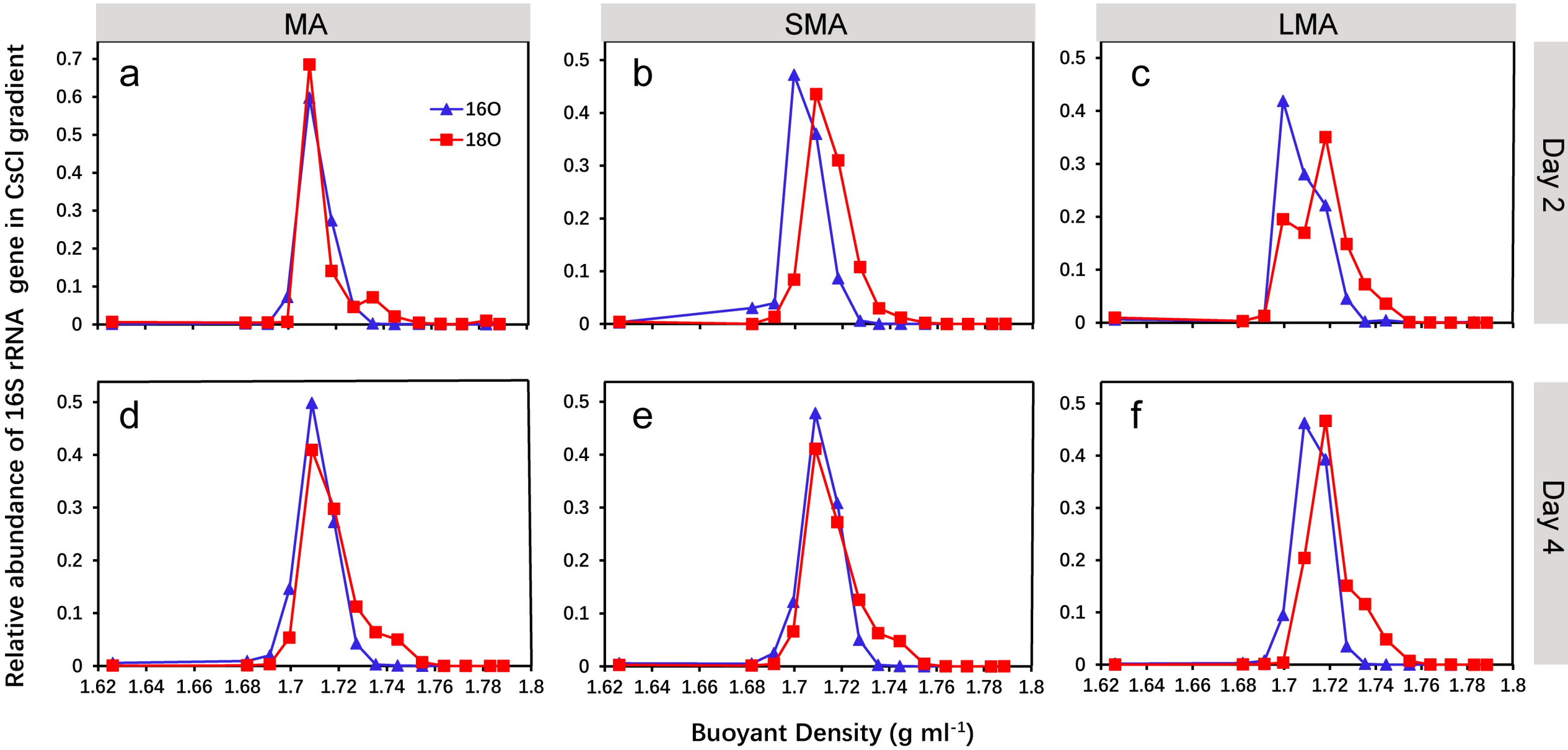
MA
SMA
LMA
a
b
c
d
e
f
16O
18O
Day 2
Day 4
Relative abundance of 16S rRNA gene in CsCl gradient
Buoyant Density (g ml-1)
0
0.1
0.2
0.3
0.4
0.5
0.6
0.7
1.62
1.64
1.66
1.68
1.7
1.72
1.74
1.76
1.78
1.8

Fig.2

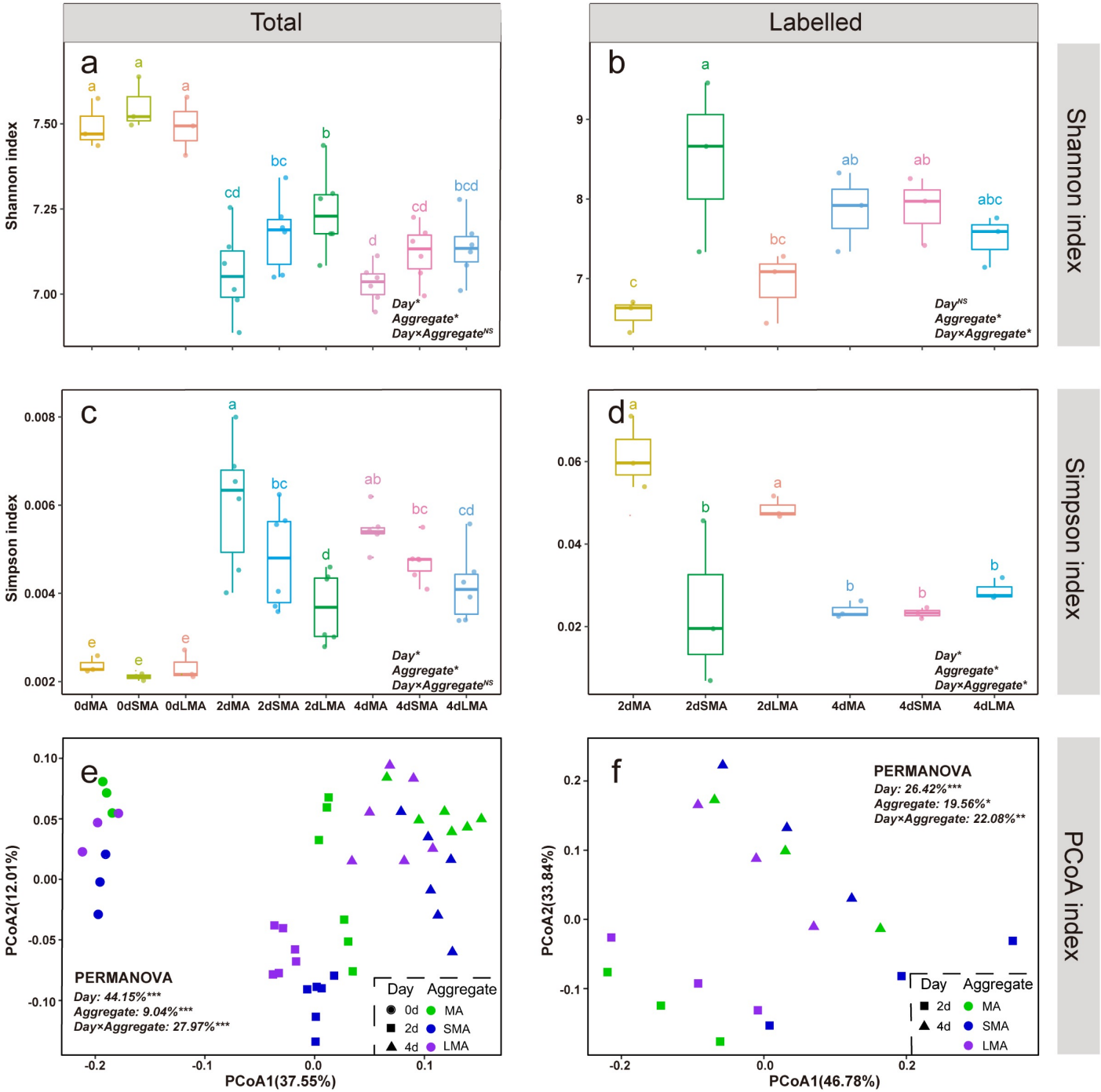
Total
Labelled
Shannon index
Simpson index
PCoA index
a
b
c
d
e
f
Shannon index
Simpson index
Day*
Aggregate*
Day×Aggregate^NS
Day^NS
Aggregate*
Day×Aggregate*
0dMA 0dSMA 0dLMA 2dMA 2dSMA 2dLMA 4dMA 4dSMA 4dLMA
2dMA 2dSMA 2dLMA 4dMA 4dSMA 4dLMA
PERMANOVA
Day: 44.15%***
Aggregate: 9.04%***
Day×Aggregate: 27.97%***
PERMANOVA
Day: 26.42%***
Aggregate: 19.56%*
Day×Aggregate: 22.08%**
Day Aggregate
0d MA
2d SMA
4d LMA
Day Aggregate
2d MA
4d SMA
LMA
PCoA1(37.55%)
PCoA2(12.01%)
PCoA1(46.78%)
PCoA2(33.84%)

Fig.3

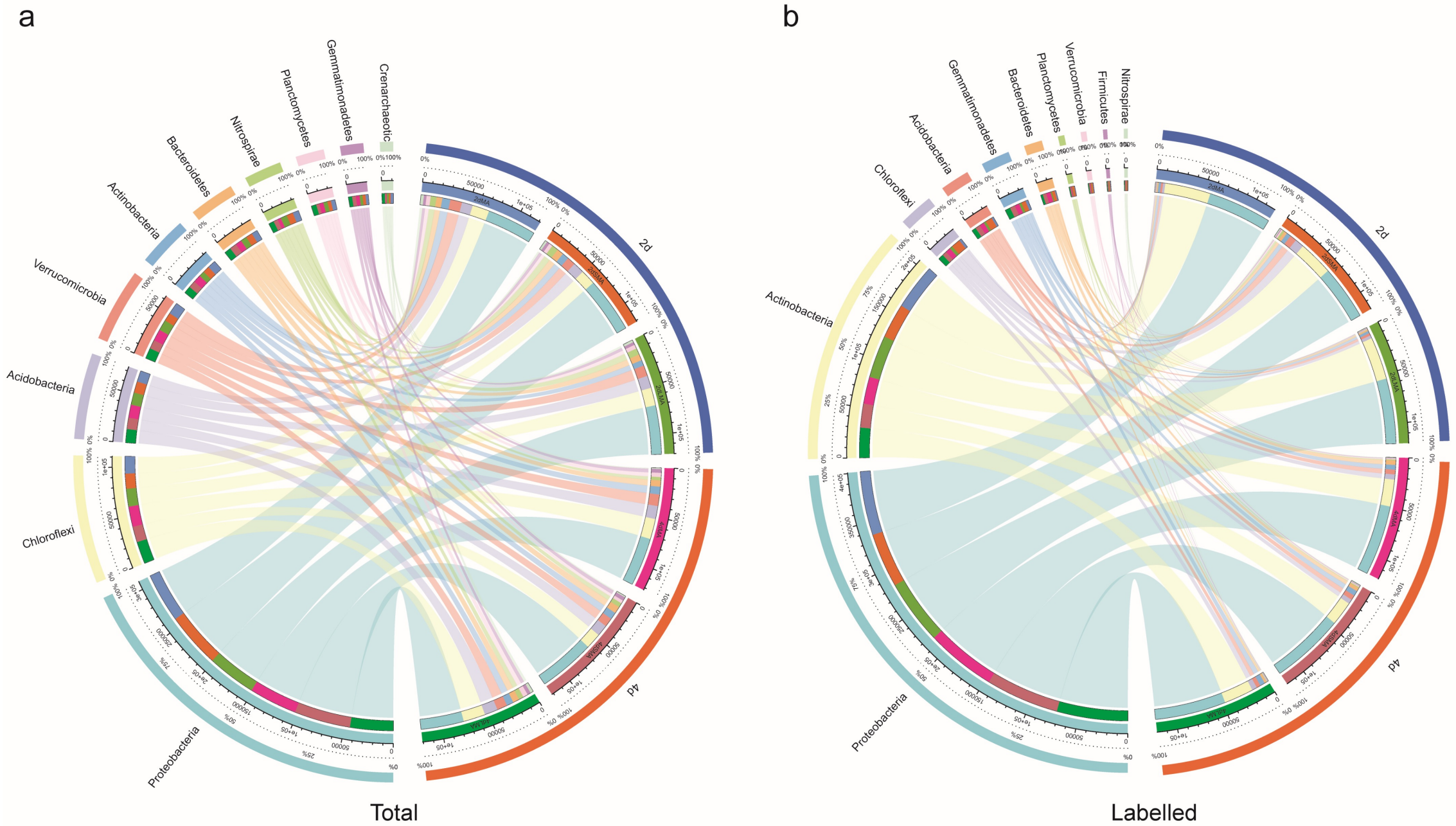
a
Crenarchaeotic
Gemmatimonadetes
Planctomycetes
Nitrospirae
Bacteroidetes
Actinobacteria
Verrucomicrobia
Acidobacteria
Chloroflexi
Proteobacteria
2d
4d
Total
b
Nitrospirae
Firmicutes
Verrucomicrobia
Planctomycetes
Bacteroidetes
Gemmatimonadetes
Acidobacteria
Chloroflexi
Actinobacteria
Proteobacteria
2d
4d
Labelled

Fig.4

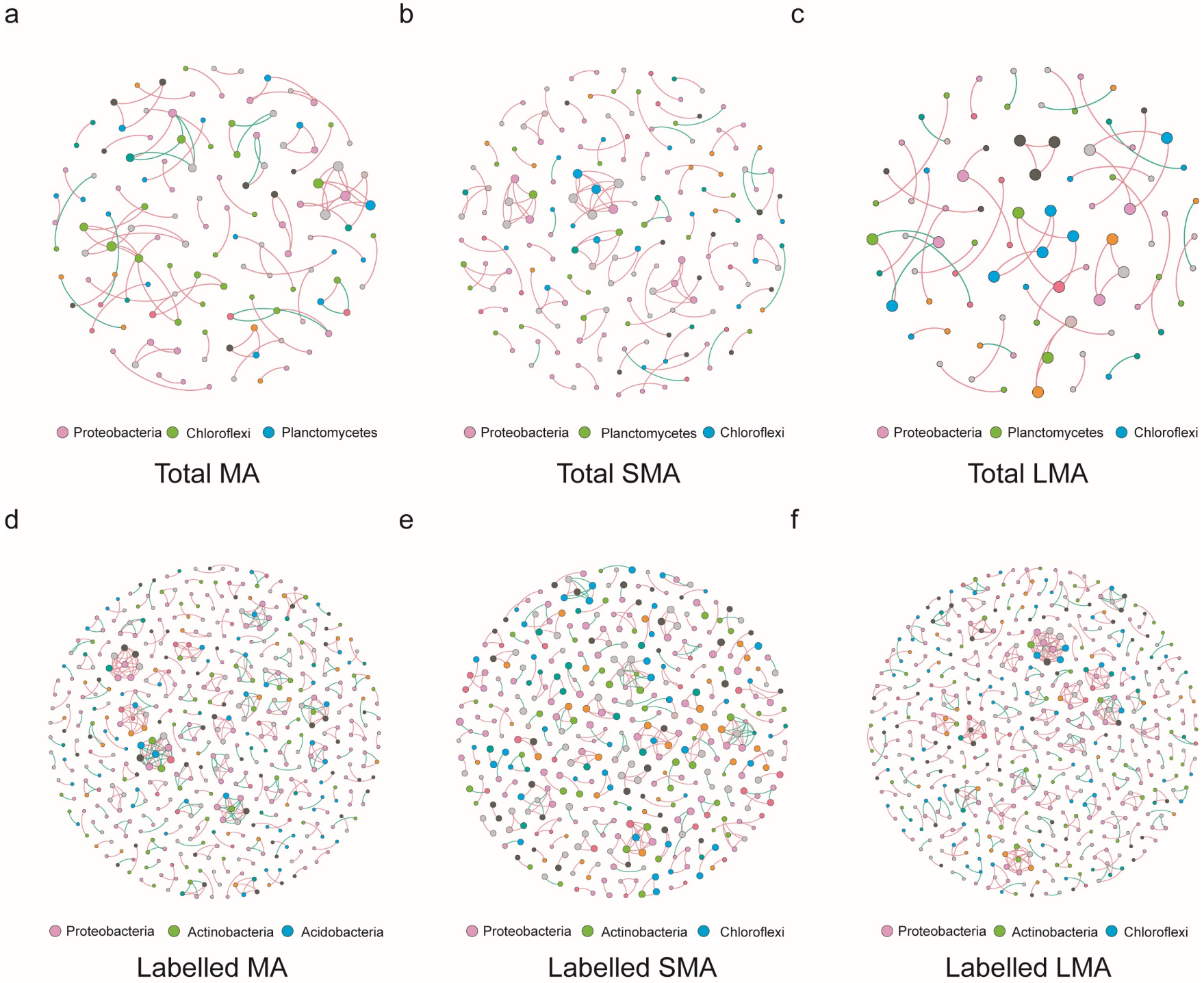
a
b
c
Proteobacteria Chloroflexi Planctomycetes
Total MA
Proteobacteria Planctomycetes Chloroflexi
Total SMA
Proteobacteria Planctomycetes Chloroflexi
Total LMA
d
e
f
Proteobacteria Actinobacteria Acidobacteria
Labelled MA
Proteobacteria Actinobacteria Chloroflexi
Labelled SMA
Proteobacteria Actinobacteria Chloroflexi
Labelled LMA

Fig.5

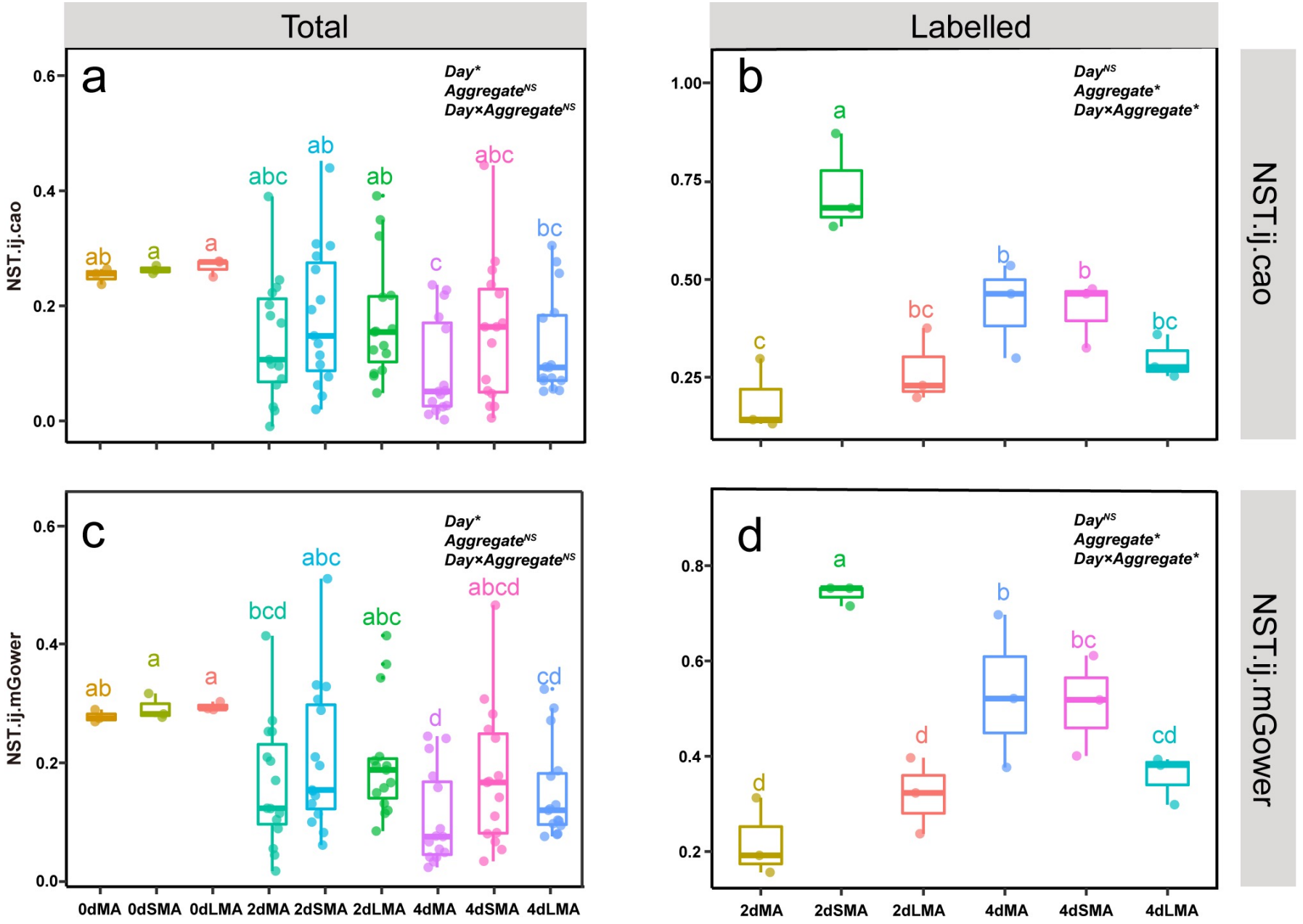
Total
Labelled
NST.ij.cao
NST.ij.mGower
a
b
c
d
Day*
Aggregate^NS
Day×Aggregate^NS
Day^NS
Aggregate*
Day×Aggregate*
0dMA
0dSMA
0dLMA
2dMA
2dSMA
2dLMA
4dMA
4dSMA
4dLMA

Fig.6

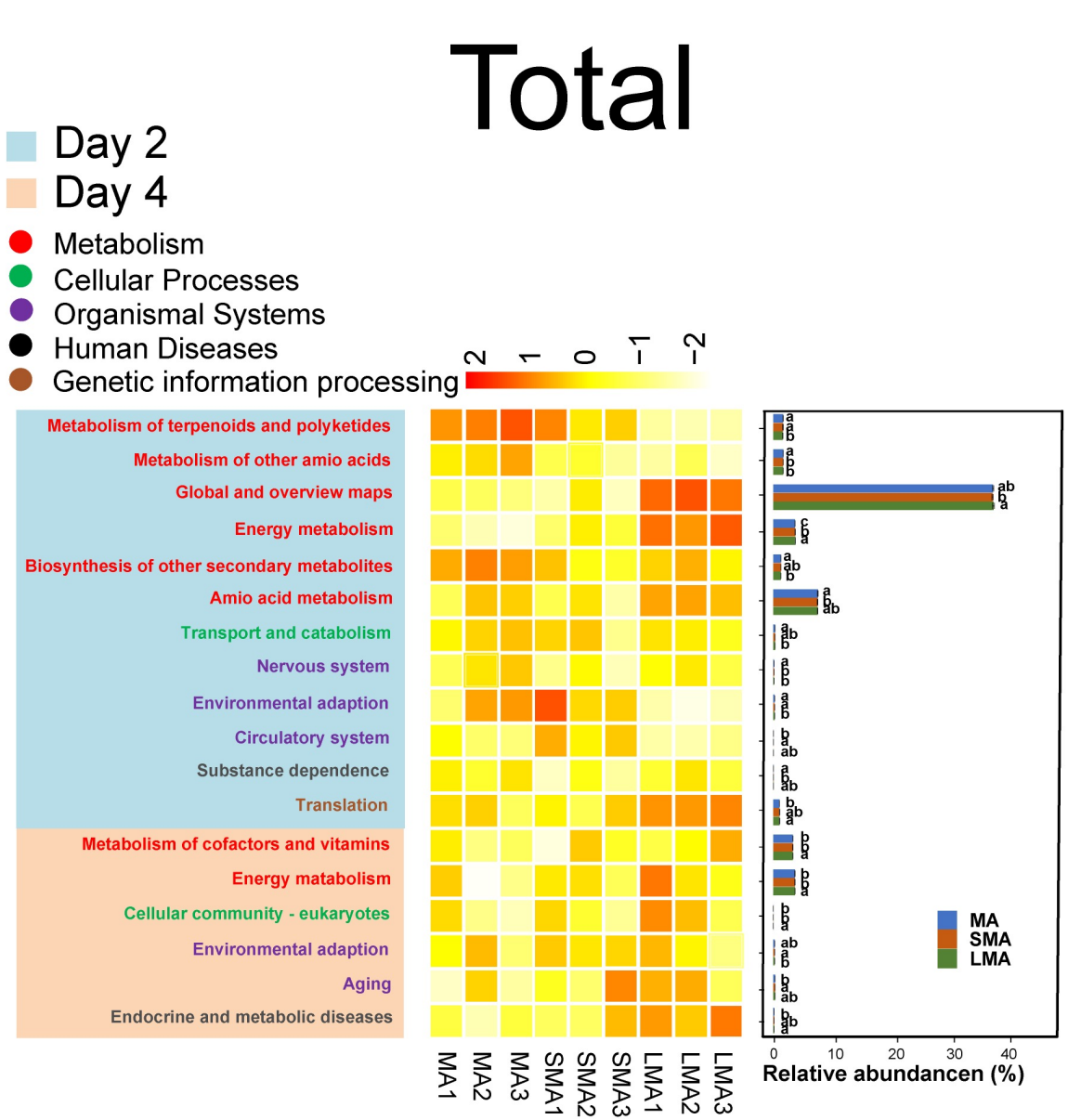
a
Total
Day 2
Day 4
Metabolism
Cellular Processes
Organismal Systems
Human Diseases
Genetic information processing
2 1 0 −1 −2
Metabolism of terpenoids and polyketides
Metabolism of other amio acids
Global and overview maps
Energy metabolism
Biosynthesis of other secondary metabolites
Amio acid metabolism
Transport and catabolism
Nervous system
Environmental adaption
Circulatory system
Substance dependence
Translation
Metabolism of cofactors and vitamins
Energy matabolism
Cellular community - eukaryotes
Environmental adaption
Aging
Endocrine and metabolic diseases
MA1 MA2 MA3 SMA1 SMA2 SMA3 LMA1 LMA2 LMA3
MA
SMA
LMA
0 10 20 30 40
Relative abundancen (%)

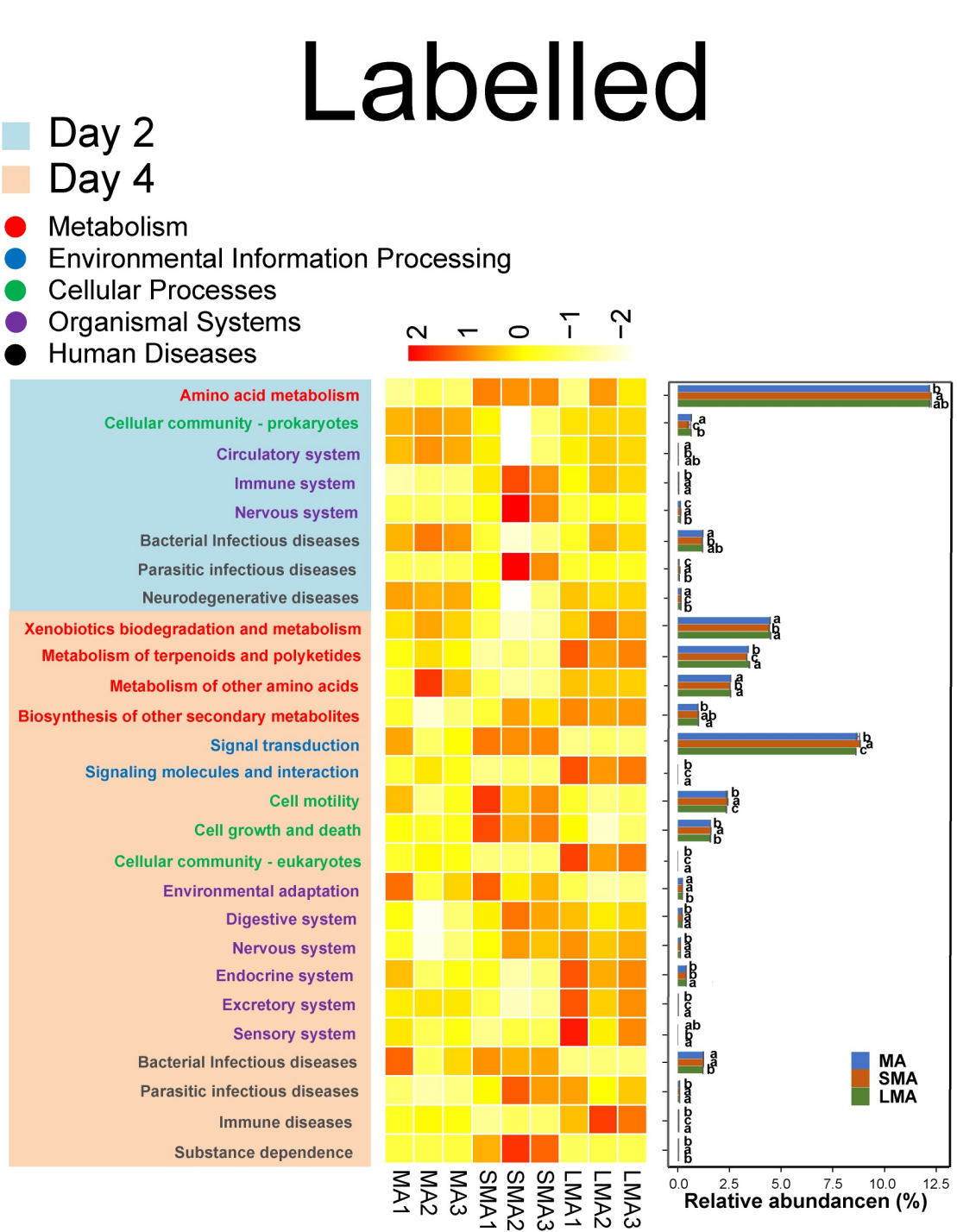
b
Labelled
Day 2
Day 4
Metabolism
Environmental Information Processing
Cellular Processes
Organismal Systems
Human Diseases
2 1 0 −1 −2
Amino acid metabolism
Cellular community - prokaryotes
Circulatory system
Immune system
Nervous system
Bacterial Infectious diseases
Parasitic infectious diseases
Neurodegenerative diseases
Xenobiotics biodegradation and metabolism
Metabolism of terpenoids and polyketides
Metabolism of other amino acids
Biosynthesis of other secondary metabolites
Signal transduction
Signaling molecules and interaction
Cell motility
Cell growth and death
Cellular community - eukaryotes
Environmental adaptation
Digestive system
Nervous system
Endocrine system
Excretory system
Sensory system
Bacterial Infectious diseases
Parasitic infectious diseases
Immune diseases
Substance dependence
MA1 MA2 MA3 SMA1 SMA2 SMA3 LMA1 LMA2 LMA3
MA
SMA
LMA
0.0 2.5 5.0 7.5 10.0 12.5
Relative abundancen (%)